Journal Pre-proof

Lower Jurassic felsic diatreme volcanism recognized in central Patagonia as evidence of along-strike rift segmentation

Leonardo Benedini, Cecilia Pavón Pivetta, Paulo Marcos, Daniel A. Gregori, Mercedes Barros, Nicolas Scivetti, Anderson Costa Dos Santos, Leonardo Strazzere, Mauro Geraldes, Teodoro de Queiroz Bernabé

PII: S0895-9811(20)30248-0

DOI: https://doi.org/10.1016/j.jsames.2020.102705

Reference: SAMES 102705

To appear in: *Journal of South American Earth Sciences*

Received Date: 26 November 2019

Revised Date: 12 June 2020

Accepted Date: 14 June 2020

Please cite this article as: Benedini, L., Pivetta, Cecilia.Pavó., Marcos, P., Gregori, D.A., Barros, M., Scivetti, N., Dos Santos, A.C., Strazzere, L., Geraldes, M., de Queiroz Bernabé, T., Lower Jurassic felsic diatreme volcanism recognized in central Patagonia as evidence of along-strike rift segmentation, *Journal of South American Earth Sciences* (2020), doi: https://doi.org/10.1016/j.jsames.2020.102705.

This is a PDF file of an article that has undergone enhancements after acceptance, such as the addition of a cover page and metadata, and formatting for readability, but it is not yet the definitive version of record. This version will undergo additional copyediting, typesetting and review before it is published in its final form, but we are providing this version to give early visibility of the article. Please note that, during the production process, errors may be discovered which could affect the content, and all legal disclaimers that apply to the journal pertain.

© 2020 Published by Elsevier Ltd.

Journal Pre-proof

LOWER JURASSIC FELSIC DIATREME VOLCANISM RECOGNIZED IN CENTRAL PATAGONIA AS EVIDENCE OF ALONG-STRIKE RIFT SEGMENTATION.

Leonardo Benedini [a], Cecilia Pavón Pivetta[b], Paulo Marcos[a], Daniel A. Gregori [a], Mercedes Barros [a], Nicolas Scivetti [e] Anderson Costa Dos Santos[c*], Leonardo Strazzere[d], Mauro Geraldes[c],. Teodoro de Queiroz Bernabé [f]

a Cátedra de Geología Argentina, Departamento de Geología, Universidad Nacional del Sur and INGEOSUR, San Juan 670, 8000 Bahía Blanca, Argentina.

b Cátedra de Geología de Yacimientos, Departamento de Geología, Universidad Nacional del Sur and INGEOSUR, San Juan 670, 8000 Bahía Blanca, Argentina

c Universidade do Estado do Rio de Janeiro, Faculdade de Geologia, Departamento de Mineralogia e Petrologia Ígnea. Rua São Francisco Xavier, 524, Maracanã, Rio de Janeiro, Brasil – CEP: 20.550-900. * https://orcid.org/0000-0003-2526-8620 - - Tektos Group and Instituto GeoAtlântico (UERJ, Brazil) /Geobiotec, Departamento de Geociências, Universidade de Aveiro, 3810-193 Aveiro, Portugal.

d Cátedra de Geología Minera, Departamento de Geología, Universidad Nacional del Sur and INGEOSUR, San Juan 670, 8000 Bahía Blanca, Argentina.

e Cátedra de Geofísica, Departamento de Geología, Universidad Nacional del

Sur and INGEOSUR, San Juan 670, 8000 Bahía Blanca, Argentina.

f Universidade do Estado do Rio de Janeiro

Journal Pre-proof

Journal Pre-proof

Abstract

The early Jurassic volcanism of Central Patagonia covers an extensive area of 50,000 km^2 where the volcanic deposits occur as isolated systems. The volcanic records form an elongated belt in which the composition, depositional and genetic features, show several differences along with its distribution. The Cañadón Chileno Complex (CCHC), located in the Río Negro province, provides the opportunity to evaluate and improve the knowledge about the Lower Jurassic volcanic stratigraphy and the lower Jurassic regional setting of Central Patagonia.

Based on the field and laboratory data developed in the present work, 22 lithofacies were recognized and grouped into eight facies associations. The continental sedimentary environments include alluvial fan deposits (FA 1), ephemeral deposits (FA 2), braided fluvial deposits (FA 3), alluvial plains, or over banks (FA 4), and lacustrine deposits (FA 9). On the other hand, the pyroclastic facies were separated according to the pyroclastic currents involved during the deposition; into fall-out, dilute, and density currents (FA 5, FA 6, and FA 7). Effusive andesitic feeders and lava-flows (FA 8) were also recognized.

The stratigraphic data obtained in the present work allow proposing the existence of two felsic diatreme volcanoes in the CCHC records - described here as Southern and Northern Zone-, developed over a local subsided area, represented by an asymmetrical basin.

Seven units were recognized and described in the CCHC (Units a, b, c, d, e, f, and g: unit (a) represents an initial stage of continental sedimentation recorded throughout the entire Complex. Unit (b) represents the upper felsic diatreme facies, in Southern Zone of the Complex, where debris flows are interbedded with massive

Journal Pre-proof

lapilli-tuff deposits. Unit (c) consists of local andesitic lavas flows and feeder dikes, and the unit (d) consists of welded lapilli tuff deposits interpreted as the growth of the volcanic system. The Northern Zone evolves similarly with the felsic intra-diatreme deposits of unit (e). The unit (f) consisting of an effusive stage represented by extended andesitic lava flows. Finally, a deep lacustrine system is installed (unit g) that includes shallow and deep facies, with intercalations of local pyroclastic deposits.

Also, new geochronological data (U-Pb zircon age of 188 ± 3 Ma) was determined to confirm and reinforce the correlation criteria between the different volcanic areas in Central Patagonia, indicating that the volcanism described here is synchronous with the Northern silica-rich calderas of the Garamilla Formation as well as the large andesitic volcanoes of the Lonco Trapial Formation located southward to the CCHC. The regional volcanism changes described, in the present work, are connected with the N-S rift segment limited by E-W regional transfer fault systems developed in continuity to the strike-slip structures of the La Esperanza area.

Journal Pre-proof

1. Introduction

The Jurassic magmatism in the eastern region of Patagonia is usually assigned to the Chon Aike Igneous Province. It forms one of the largest rhyolitic province in the world (Pankhurst *et al*. 1998, 2000; Riley *et al.* 2001) and a significant geological feature of North Patagonia. Its origin is related to the rupture and fragmentation of SW Gondwana with the subsequent generation of the South Atlantic Ocean (Rapela *et al.* 2005 and references therein). A combined roll-back subducted slab in the Pacific margin, and the asthenospheric upwelling in the foreland area characterizes the massive extension of the Patagonian crust and the widespread volcanism developed during this time-spam (Pankhurst *et al*. 2000; Rapela *et al.* 2005; Mpodozis and Ramos, 2008). Recently, Navarrete *et al.* 2016 and 2019 have proposed the existence of compressive stages in Patagonia and their relationship with the Chon Aike SLIP location and evolution.

The Central Patagonia area is one of the portions of the Patagonia region, where its magmatism is extensively recorded (Fig. 1). The Jurassic outcrops form a 450 km elongated belt, orientated NNW-SSE, that covers more than 50,000 km^2, named as Central Patagonia Belt (CPB; Zaffarana *et al.* 2018). The CPB occurs in the back-arc environment, respect to the western short-lived Early Jurassic arc (Subcordilleran Plutonic Belt; Gordon and Ort, 1993; Haller *et al.* 1999; Rapela *et al.* 2005). The CPB volcanic products were usually undifferentiated in the literature; however, local and regional geological data indicates that the related records are far from being homogeneous.

The CPB volcanic units can be divided into two compositional domains related to different stacking patterns. The North domain located mainly in the Río Negro

Province is characterized by calc-alkaline silica-rich pyroclastic deposits associated with caldera-forming eruptions (Benedini and Gregori, 2013; Benedini *et al*. 2014). The South domain, mainly developed southern to the 41º30' S parallel, is composed of calc-alkaline highly-extended intermediate to basic lavas (Lonco Trapial formations, Lesta and Ferello, 1972; Nullo and Proserpio, 1975; Nullo, 1978) and minor sedimentary deposits (Proserpio, 1978; Page and Page 1993). The compositional change of volcanic records between both domains shows a transition interval where both coexist together along 110 km (between 40º30 to 41º30).

In order to understand how such regional changes occur, a detailed geological description in a volcano-sedimentary depocenter named Cañadón Chileno Complex (CCHC) was made. The CCHC occurs as an elongated volcano-sedimentary depression, 90 km eastward of San Carlos de Bariloche city. This work attempts to point out the changes in the local geology as a function of the spatial distribution of the CPB units, besides analyzing the relationships of such variations with the regional setting. New geologic fieldwork description, mapping, and geochronological data are combined here to set up a detailed tectonic configuration of the Lower Jurassic Patagonian Volcanism.

2. Tectonic settings

The Gondwana break-up in Argentina is marked by a widespread extension manifested through the formation of extensive rift systems that were active during the Triassic and Jurassic Period. The extensional phase was oblique respect to the NNW-oriented inherited structural weakness basement (Uliana and Biddle, 1988). The Lower Jurassic oblique extension was reported in western Argentina, over more than 800 km, related to the syn-rift units of the Neuquén basin (Neuquén Province,

Cristallini *et al.* 2009; Bechis *et al.* 2014) and Central Andes (Mendoza Province, Bechis *et al.* 2009).

In North Patagonia, the Gondwana break-up records are coeval with the oblique roll-back of the subducted slab (Rapela *et al.* 2005; Mpdozis and Ramos, 2008). The Pacific subduction (Gordon and Ort, 1993; Haller *et al.*1999; Rapela *et al.* 2005) formed a discontinuous magmatic arc in the Patagonian Andes, with sparsely distributed granitic bodies (Rapela *et al.* 2005). Eastward, in the extra Andean region, the CPB also registered the oblique extension event that is represented by a Lower Jurassic high obliquity rift system in the vicinity of the Limay River (Benedini *et a*l. 2014).

In the North CPB domain, oblique extension and the related volcanism extends from Piedra del Águila to Ingeniero Jacobacci (Benedini *et al.* 2014; Fig. 1) covering more than 150 km along N345° strike. The Lower Pliensbachian Garamilla Formation (~187 ± 2 Ma, U-Pb zircon age, Benedini and Gregori, 2013) registers this extensional phase. Several silica-rich caldera-forming eruptions took place together with a large number of volcanic centers and a widespread dike swarm. The regional dike swarm within Garamilla Formation progressively disappears before the Fita Ruin Canyon, 80 km southward Piedra del Aguila city. The dike swarm is markedly continuous, tracing the regional stress field and the obliquity angle of extension ~70° (Benedini *et al.* 2014).

The CCHC occurs in a transitional CPB domain southern to the Fita Ruin Canyon, where acidic and intermediate volcanic systems coexist up to the 41°30’ S parallel. In this interval, the pyroclastic silica-rich deposits are gradually replaced by the basic to intermediate volcanic deposits that characterizes the South CPB domain.

Journal Pre-proof

The South CPB domain geological record is represented by the Lonco Trapial Formation (Lesta and Ferello, 1972; Nullo and Proserpio, 1975), which is composed by calc-alkaline intermediate to basic lavas (Lesta and Ferello, 1972; Nullo and Proserpio, 1975; Zaffarana et al., 2018) and minor sedimentary deposits (Proserpio, 1974; Page and Page, 1993). It is formed by one of the most productive andesitic volcanism in Patagonia (Taquetrén hill, near to the Chubut and Río Negro provinces boundary). This unit, temporarily coeval to the Garamilla Formation, yielded 190-183 Ma (Zaffarana and Somoza, 2012; Cúneo *et al.* 2013) between the Pliensbachian and the early Toarcian ages.

A second extensional phase is recorded in the South CPB domain, and it is represented by pull-apart sedimentation (Cañadón Asfalto Formation) during the Toarcian and Bajocian ages (Bouhier *et al.* 2017; Hauser *et al.* 2017). Continental fluvial and deep lacustrine sedimentary rocks were deposited interdigitated with andesitic and dacitic lavas (Figari and Courtade, 1993; Cortinas, 1996; Cuneo *et al.* 2013; Figari *et al.* 2016; Hauser *et al.* 2017; Bouhier *et al.* 2017). The dacitic ignimbrites facies are subordinated to the effusive ones (Figari *et al.* 2016; Bouhier *et al.* 2017).

A summary of tectonics elements, including those registered in the Atlantic Ocean area, together with locations, ages, geological units, and rifting episodes, is presented in Table 1 following similar criteria to Pankhurst *et al.* 2000.

3. Applied Methodologies

A total of six stratigraphic sections were logged during fieldwork. Because lateral variability is ubiquitous, 312 observation points were registered to describe the different architectural elements. The recorded logging data include grain sizes,

Journal Pre-proof

lithofacies codes, sedimentary structures, component abundances, and paleocurrent information. Lithofacies coding of volcanic rocks was elaborated following Branney and Kokelaar (2002) and McPhie *et al*. (1993) and for sedimentary facies following Miall (1996). Representative samples were collected for petrographic descriptions. Strata and fault attitudes, as well as thickness, were measured together with the facies analysis.

Thirty-one thin sections were made in the Laboratorio de Petrotomía at the Universidad Nacional del Sur, Argentina (UNS), to determine volcanic and sedimentary textures besides mineralogy. Likewise, we establish the depositional age of the CCHC volcanic deposits, sample PRJ-FA84, in the Laboratório Multiusuário de Análises Isotópicas (MultiLab) at Rio de Janeiro State University (UERJ), Brazil. An ICP-MS laser ablation Neptune Plus was used to determine the U-Pb isotopic concentrations in zircons.

4. Results

4.1. Field descriptions

The CCHC outcrops are elongated, extend along *ca.* 6km, and 'sigmoid-shaped'. It is bounded by two normal fault arrays, NNW-SSE strike, that extend beyond the CCHC limits. According to the structural framework, bed attitude, stacking pattern, and the changes in environmental conditions, the CCHC records can be divided into two different zones (Northern and Southern) that are genetically linked to a common origin and exposed in angular unconformity over Lower Permian granites.

Journal Pre-proof

The Northern Zone of the CCHC presents a 4 km diameter, measured on the major axis of the ellipse, and shows an elliptical morphology in which the volcanic beds have centripetal inward immersions (saucer-shaped). These attitudes are interpreted as generated under the influence of both syn-volcanic activity and post-depositional deformation. Conversely, the Southern Zone has a minor extension (*ca*. 1.5 km diameter) and is locally faulted and folded. The constrained deformation of the deposits indicates that the deposition in both zones occurs diachronically. Particularly, volcanic sedimentation begins in the southern zone and subsequently migrates northwards with the evolution of the Complex (Fig. 2).

According to the collected data, 22 sedimentary and volcanic facies were recognized and characterized (Table 2). The sedimentary deposits were grouped into five facies associations (FAs) denominated as FA 1, FA 2, FA 3, FA 4, and FA 9 while the volcanic units were divided into four facies associations (FA 5, FA 6, FA 7and FA 8). The continental sedimentary environments include alluvial fan deposits (FA 1), ephemeral deposits (FA 2), braided fluvial deposits (FA 3), alluvial plains, or over banks (FA 4), and lacustrine deposits (FA 9). On the other hand, the pyroclastic facies were separated according to the pyroclastic density currents primary processes; into direct fall-out dominated, traction-dominated, and granular flow-dominated facies association (FA 5, FA 6, and FA 7). The effusive andesitic feeders and lava-flows (FA 8) were considered as a unique FA (Table 3). Figures 3 and 4 show the relationships between the different FAs.

The FAs are grouped into six sedimentary and volcanic units. The first one, unit (a), is recorded in both zones (Northern and Southern). The units (b), (c), and (d) crop out in the Southern Zone, while units (e), (f), and (g) occur in the Northern Zone. All of them compose the entire CCHC stratigraphic sequence. The FAs

Journal Pre-proof

distributions, relationships, and occurrence in the CCHC zones are shown in figures 3 and 4.

4.2. The CCHC pre-eruptive stratigraphy

The unit (a) crops-out along the western margin of the Complex (~ 6km) being covered by modern deposits and unit (b) facies. It consists of a 40 to 130m thick fining-upward sequence of continental deposits (Fig. 5A). The alluvial fans FAs (FA 1) grades to ephemeral and overbank deposits while sedimentation progresses eastward from the western fault scarp, as indicated by paleocurrent data. The unit thickness also diminishes in the same direction. The FA 1 and FA 2 dominate the basal sequence record, while FA 4 is only poorly represented toward the top of the Unit.

The alluvial fan record (FA 1) is red and white-colored, and this feature allows its differentiation from the upper volcanic associations. Massive matrix-supported conglomerate and breccia (gmm) are the most significant facies in this association. It forms a flat to lobe-shaped strata of 0.1 to 5 m thick, characterized by an erosive base, occasionally channelized (gcm, gt), and normally graded (gmg; Fig. 5B).

Channel shaped sandstone bodies (FA 2a) are constituted by massive sandstones (Sm) 1 to 6 m thick and 5 to 50 m wide. Occasionally normal-coarse-graded conglomerate (gmg) occurs at the base of the unit (Fig. 5C). The massive sandstones are homogeneous, moderately to poorly sorted, and coarse to medium-grained. The lobe-shaped sandstone bodies (FA 2b) also occur at the base of unit (a), presenting 0.5 to 2 m thickness, and extend laterally for more than 30 m. The sand body tops are concave or flat, whereas the base is undulated or eroded,

Journal Pre-proof

sometimes formed by laminated siltstones (fl). Mud clasts up to 3 cm diameter can be found at the base (Fig. 5D).

The fluvial braided deposits (FA 3) are poorly exposed and are characterized by an erosive concave-up base. Each unit exhibits a sharp to the concave-up base and concave-down top, resulting in an overall wing-shaped geometry. They comprise white-colored, well-sorted, fine to medium-grained sandstones. Internally, it can be subdivided into different sets or bedforms (0.1 to 1.5 m thickness), showing Sp, Sh, Sl, and Sr (Fig. 5E). The prograde direction is N30° and can be measured in the outcrops. Ripple lamination (Sr) is scarcely observed.

As it was previously described, to the top of the sequence, the ephemeral fluvial deposits (FA 2) are gradually replaced by fine-rich overbank or alluvial plains deposits (FA 4; Fig. 5G). These facies consist of 0.1 m up to 10 m thickness composed of fine-grained red to grey laminated and massive mudstone deposits that can be followed laterally for 70 meters in strike directions (Fig. 5F). However, lateral facies distribution can be modified by the effects of pyroclastic cut and fill relationships.

4.3. The stratigraphy of the Southern Zone of CCHC

The occurrence of unit (b) is marked by a change in the stacking pattern, lithology, environment, and architectural style. The conglomerates and sandstones units that characterize the basal sequence of unit (a) are replaced by dominantly pyroclastic deposits interbedded with minor fluvial sedimentation. Unit (b) thickness varies between 90 m and 170 m; the pyroclastic density current deposits characterized the lower section (FA 7a) interbedded with conglomerate and

Journal Pre-proof

sandstone beds (FA 1 and FA 2b). Upward the top of the unit (b), the deposit changes to entirely pyroclastic composition.

The pyroclastic facies are typically white to grey colored and composed of stratified lapilli-tuff (FA 6) and dominant pumice-rich massive lapilli-tuff (FA 7a; Fig. 6A). The FA 6 are scarcely represented, moderately sorted, and show bed-load structures (low angle cross-stratification). Facies thickness varies between 0.5 to 2 m and has been traced laterally for more than 250 m. However, the vertical separation of massive lapilli-tuff units is highly complex. The modal composition, in thin section, reveals that these facies vary from dacitic to rhyolitic.

The massive lapilli-tuffs are poorly to unwelded deposits with a juvenile fragment concentration that varies between 35-60% in volume. The accidental fragments are found in low concentrations (0-20%) and are less abundant in the latest pyroclastic pulses. The lithic fragments size gives the most remarkable features of the deposits. It consists of sandstones and conglomerate blocks that range from 1 to 70 cm in diameter (Fig. 6B). The sedimentary blocks are sub-angular, radial-fractured with cross-hatched designs indicating the influence of volatile expansion by thermal effects. Also, bread-crust texture, pillow textures, and microperlitic fractures are usual and occasionally related to its muddy appearance in the massive lapilli-tuff facies (Fig. 6C). The FA 7a contacts are usually vertical and sharp (Fig. 6D).

Several sedimentary levels of FA 1 and FA 2 were recognized within the unit (b) lower sequence (Fig. 6E). The sandstones and conglomerates clasts are subangular and almost exclusively of wall-rock granitic composition. These high energy deposits cut the underlain facies in erosional and basal sharp contacts. Syn-

Journal Pre-proof

eruptive layers thickness varies between 0.25 to 1 m, indicating that the sedimentary strata became progressively thinner compared with the previous unit (Fig. 6F). The upper section of unit (b) is formed by juvenile-rich massive pyroclastic deposits (FA 7a; 45-60%), without evidence of quench-cooling textures. The thickness increases significantly to the upper section of unit (b), as well as the juvenile fragment concentration. These deposits are markedly homogeneous, lobe-shaped, scarcely welded, and developed thickness up to 150m.

Unit (c) is composed of andesitic feeders, lava flows, and block and ash deposits. The effusive facies is separated based on their morphology and flow-banding orientation (Fig. 7A). The feeder outcrops form sub-rounded and tabular dike-shaped bodies with vertical flow bands (Fig. 7B). In contrast, the horizontal flow banded andesite (fbA) facies is the main feature of the andesitic lava flows. Lavas extend for several tens of meters along-strike with a thickness that varies from 5 to 20 m. Flow banding textures are also recognized under the microscope (Fig. 7C). The dikes intrude the early pyroclastic deposits, are fine-grained, brown to gray colored, and range between 0.5 to 2 m (FA 6 - not included in the profiles). The block and ash deposits consist of poorly sorted, monolithological, andesitic, massive tuff-breccia (FA 7b) of 5 to 10 m thickness, capping in erosional contact the earliest pyroclastic deposits.

The upper section of the Southern Zone is represented by the unit (d) that is formed by 20 to 30 m of two highly welded juvenile rich massive lapilli-tuff facies (FA 7a). These deposits are orange-colored, moderately to poorly sorted, and are separated by thin inter-eruptive fine sediments with desiccation cracks that reach up to 0.5 m (FA 4a; Fig. 7D) and cover the block and ash deposits with erosional contact. The first Ignimbrite unit presents an altered coarse surge deposit (FA 5) at

Journal Pre-proof

the base (Fig.7E and 7F). Isolated lacustrine laminated limestone outcrops were recognized and correlated with the inter-eruptive level.

4.4. Stratigraphy of the Northern Zone of CCHC

The stratigraphic record of the Northern Zone was developed after Southern sequences had been formed. The unit (e) marks the beginning of the Northern sequence and is composed of compound massive lapilli tuff facies (FA 7a; Fig. 8A). The pyroclastic deposits overlay the pre-eruptive sedimentary beds (unit (a)) with mostly covered contacts. Consist of highly-welded grey to white-colored, lithic poor (5-15%), eutaxitic massive lapilli-tuff. Water influence in the pyroclastic record is also registered, such as observed in concentric fractured-fragments, accretionary lapilli, and microperlitic textures (Fig. 8B and 8C).

The pyroclastic record includes three units that vary between 60 to 140 m, giving a combined thickness of 350 m. These deposits are separated by moderately preserved inter-eruptive fine-grained facies that reflect the influence of post-depositional reworked (FA 4), hiding the limits between these units. Discrete levels of surge deposits also occur in this unit (Fig. 8D). It shows moderate sorted sets organized in thin parallel beds varying between 1 to 20 cm thick (L//s and LTds) with low angle (< 15 °) and cross-stratification (Lxs). Free crystals vary between 7 and 15% of the total rock, while lithic fragments accessory are recorded in moderate to high concentrations (18-40%). Diluted pyroclastic density current deposits register syn-volcanic ballistic impacts formed by 20 to 35 cm volcanic blocks (Fig. 8E). The outcrops are 1 to 7 m thick, gray to pink color, and form tabular units with erosional base. Subaerial deposition can generate cracked tuff matrix and oxidation.

Journal Pre-proof

Unit (f) marks a substantial change in volcanic activity; the lower section develops a significant effusive stage formed by extended andesitic lava flows, while the upper section consists of block and ash flow deposits. The lower section is formed by two andesitic lava flows, 150 m thick, laterally spread out, and elliptical funnel-shaped. The upper section, on the other hand, presents two extended monolithological (andesitic) massive tuff-breccia (mTBr) interbedded with massive lapilli-tuff (Fig. 9A). The mTBr reaches up to 15 m and has more than 2 kilometers of lateral extension. The origin of mTBr deposits is considered to be related to lava collapses and the generation of a block and ash deposit.

The unit (g) crops out at the top of the CCHC. It covers, in erosive contact, the previously described pyroclastic deposits. It consists of a 5-20 m thick discrete eruption of welded massive lapilli-tuff, interbedded with silicified and bituminous limestones. Lacustrine facies (FA 9a and FA 9b) occur together, forming two different levels that reach up to 30 m and show shallow and deep facies interbedded with minor channelized sandstones beds (FA 9a, FA 9b, FA 4, and FA 3). The lacustrine facies show a tabular morphology, strongly dipping (35°), that extends for more than 1 km normal of dip-direction and an elliptical distribution (Fig. 9B). It has grey to white color and forms 1.5 m thick beds of undulose laminated algae-related micritic limestones of 0.1 to 10 mm thick.

Lacustrine facies were strongly affected by post-depositional phenomena. Silica-rich fluids migration was recognized as fractures infill that generates nodular and lenticular chert layers. The silica-rich layers can grow laterally, forming uniform silcretes and massive nodules. The FA 9b consists of parallel thin laminated limestones, without undulose stratification (Fig. 9C). The laminae are 0.1 to 5 mm

Journal Pre-proof

thick, very good sorted, mainly of organic matter-rich micrites and fetid smell on fresh cuts with unidentified plant remains (Fig. 9D),

The pyroclastic activity is also recorded at the top of unit (f) as matrix-supported, either non-graded or stratified, poorly sorted polymictic breccia with variable block concentration (30-45%; FA 9c). The lithofacies form an up-cone shaped outcrop of 2-10 m thick and 0.75 km^2 area with a diffuse vertical arrangement that gives it a distinctive positive morphology (Fig. 9E). It consists of lithic angular to sub-angular breccia size blocks immersed in a coarse-grained tuff matrix. Breccia blocks are 3 to 60 cm in diameter and are formed by andesitic lava, mudstones, limestones, tuff, and juvenile fragments. An orange rhyolitic to white-colored massive lapilli-tuff crowns the CCHC upper succession. It is 25 m thick and shows a low concentration of lithic fragments.

5. Geochronology

In order to obtain an accurate age of the CCHC, zircons from a massive eutaxitic lapilli-tuff of unit (e) were analyzed (sample FA 84 - 40°52' 24.12"S°, 70° 8' 29.95"W). The initial sample preparation was developed in the Laboratorio de Petrotomía, Universidad Nacional del Sur (UNS). Heavy minerals were concentrated by hand panning and dense liquids. The zircons were extracted by hand-picking and mounted on a double-sided tape forming groups of 30 crystals. At the MultiLab of the Universidad do Estado do Río de Janeiro (UERJ) crystals were placed in molds with epoxy resin and polished to expose the crystals grains. Once polished, cathodoluminescence images were obtained in a scanning electron microscope. The images were used to determine the crystal´s internal structures in order to define the

Journal Pre-proof

areas to be analyzed. Once defined, 24 in situ analyses were performed using a Teledyne *Analyte G2 Excimer* Laser Ablation System coupled to a Thermo Scientific *Neptune Plus* MC-ICP-MS using the laboratory procedures (Geraldes *et al.* 2015 and Costa *et al.* 2017). The uncertainties in isotopic ratios and age for individual analyses are two sigma level, and the uncertainties in the calculated ages have a 95% confidence level.

The zircons observed in sample FA 84 are typically medium-grained (160-250 µm) and show euhedral morphology with a magmatic zonation (oscillatory and sectorized) and preserved the interfacial edges and faces. Intergrowth's faces and metamorphic zonation with discordant internal structures were not observed. Crystal morphology varies between thin, elongated prisms to equant grains. Cathodoluminescence images reveal a simple internal structure (Fig. 10A and 10B).

The individual age of zircons varies between 186 and 495 Ma. Older ages represent the metamorphic basement that is also exposed western of the studied area. Twelve analyses were plotted in the Concordia diagram (Fig. 10C), indicating an age of 188.6 ± 3.1 Ma with an MSWD of 0.84 and a probability of concordance of 0.85. This age indicates the crystallization timing of the zircon crystals, which is coeval with the depositional age of the ignimbrite facies. The range of older ages indicates erosion and picking of basement fragments during the volcanic events (Fig. 10D).

6. Discussion:

6.1. Felsic diatreme volcanism related to an asymmetrical continental basin.

Journal Pre-proof

The CCHC evolution begins in a continental sedimentary basin. The basin infill progressed eastward with alluvial to fluvial sedimentation (unit (a)) and registered thickening along the western margin, interpreted as differential mechanical subsidence, like a graben basin. A regular alluvial plain development and sedimentation (FA 4) along the stratigraphic sequence indicate periods where the area was active as a topographic depression or lowland throughout some temporal intervals during the different stages (Fig. 11A)

The CCHC evolution continued with the unit (b), which marks the beginning of phreatomagmatic activity in the Southern Zone, registering multiple small-sized eruptive phases. The related pyroclastic facies in the lower section of unit (b) penetrated the pre-eruptive deposits forming a sharp vertical contact, a variety of large, fractured sedimentary blocks, and quench cooling textures (Fig. 11B). These features indicate that aquifer rock blocks were incorporated within the pyroclastic deposits from the underlain units during the pyroclastic eruptions.

The lower section of unit (b) reflects inter-eruptive sedimentation by extra-basinal debris flow deposits, alluvial fan, and ephemeral deposits. Also, several exposures indicate re-sedimentation in water-rich environments. Low-temperature wet pyroclastic currents occur as unwelded deposits with muddy appearance. The increment of lithic fragments concentration can be interpreted either from shallow vertical migrations of moderate energy explosions or from a downward-migrating explosion locus that penetrated the underlying material, both processes associated with the external water availability (Houghton and Smith, 1993).

The recurrent marginal slides of wall rock debris, as identified in the lower section of unit (b). The deposits constitute a common phenomenon in bedded upper

Journal Pre-proof

diatreme deposits where the volcanic eruptions influence the local subsidence, e.g., the Paleogene Missouri River Breaks diatremes in Montana (White, 1996; White and Ross, 2011). These authors characterized the diatreme infill features and divided it into lower and upper diatreme deposits according to the depositional processes involved and bedding development.

The upper section of unit (b) incorporates a minimal amount of sedimentary material, and the subsidence does not progress, possibly, by the effects of more voluminous pyroclastic eruptions and an increase of magmatic input. The pyroclastic deposits changed from water driven to a purely magmatic eruption with an increase of the magmatic flux, evidenced by the increment of pumice fragments size and the ignimbrite facies thickening. Additionally, the high juvenile fragment concentrations (higher than 60%) can be related to the shallow fragmentation level (Tchamabe *et al.* 2016).

The diluted pyroclastic current (FA 6) and the fall-out deposits (FA 5) generally dominate the Maar-diatreme volcanic records. Nevertheless, they are not easily recognized in the Southern Zone evolution. The unit (b) records are characterized by poorly to unwelded massive to weakly stratified pyroclastic deposits with bed immersions between 25° to 5°. These deposits can be correlated with those described for the intracrater upper diatreme deposit (Lorenz *et al.* 1970; Wholetz and Sherindan, 1983; White and Ross, 2011) and considered as developed in a poorly preserved and partially faulted medium-sized volcano. We also consider that this Volcanic Complex constitutes a transitional structure between a large maar-diatreme and a small caldera, where magmatic-type activity was important during the evolution, especially of the final stages, e.g., Palladino *et al.* (2015).

After the pyroclastic episode, a degassed volcanic system leads to an effusive phase, developing several open vents (unit (c)) like feeder dikes, and andesitic lavas. The effusive bodies became progressively more viscous, and unstable, generating discrete andesitic block and ash flow deposits. The andesitic lava fragments registered in the PDC units indicate that a portion of these conduits could have been active during the later pyroclastic eruptions.

The volcanic system of the Southern Zone starts, again, the incorporation of volatiles, probably due to the influence of external water. The beginning of New eruptive volcanism (unit (d)), generated two violent juvenile-rich pyroclastic units (Fig. 11C). The compact and highly welded nature of the deposits seems to be more connected to high-temperature conditions, which usually dominates in magmatic fragmentation. This sequence shows a change in bedding dip angle that varies from 20° in the underlying deposits to subhorizontal in this facies. Equivalent changes in dip attitude are a common feature of different Maar-diatreme volcanoes, related to the stratified upper diatreme facies.

The volcanic activity ceased in the southern zone, and it is relocated about 3 km northwards, possibly due to coeval active transcurrent faulting (Fig. 11D). Morphology and sequences are different in both zones, although they share several similarities. A combination of volcanism and faulting excavated a new depressed area, and a set of small-sized pyroclastic eruptions developed (unit (e)). The gradual decrease in lithic concentration towards the top of the sequences is compatible with eruptions that penetrate less into the underlying material, indicating a progressive shallowing of the eruptive center.

Journal Pre-proof

The volcanic eruptions culminated and gave rise to an extended andesitic lava lake, represented by the unit (f) deposits (Fig. 11E). These deposits form a central elliptical funnel shape structure of 150 m thick. The lava lake size indicates an increase of magmatic flux and spots a volatile depletion in the volcanic system. In the upper section of unit (f), block and ash flow deposits indicate that lavas or lava dome grew and collapsed due to more viscous and volatile-rich magma involved.

The development of a lacustrine environment characterizes the latest evolutionary stage of the CCHC. Shallow and deep lacustrine facies are registered interbedded with minor channelized sandstones beds. Anoxia in volcanogenic lakes is frequent and related to steeped crater walls that prevent water mixing or circulation. Deep lacustrine facies commonly occur in Maar-diatreme volcanoes as, e.g., Maar steeped structures of the Central European volcanic belt and the Arizona volcanic field. Minor pyroclastic eruptions take place synchronously with the lacustrine sedimentation.

Journal Pre-proof

6.2. Configuration of the North CPB domain: from silica-rich caldera complexes to felsic diatreme volcanism.

The geochronological and stratigraphic data obtained in the present work allow us to correlate the CCHC volcanic deposit with the Garamilla and Lonco Trapial formations (~188 Ma). This correlation highlights the evolutionary differences in terms of local and regional conditions that occur at different latitudes and settings. Two areas were separated according to the volcanism type (Fig. 12A): I) Caldera complexes with regional dike swarms and II) Felsic diatreme complexes.

Journal Pre-proof

In particular, the dike swarms described in the North CPB domain develop three fracture patterns that characterize a scarcely subsided rift floor (Benedini et al. 2014). These patterns are (1) En-echelon dikes located at the rift floor valley margins, (2) Internal curved dikes disposed in the central valley and developed roughly orthogonal with the regional extension (~N 15°) and (3) dikes formed parallel to the rift margins (Benedini *et al.* 2014). Empirical models of highly obliquity describe equivalent fractures patterns in modern rift systems like the rift of Ethiopia (Clifton *et al.* 2000; Agostini *et al.* 2011; Autin *et al.* 2013; Brune, 2014).

The oblique rift extension, here, is considered to be promoted by an extensive diking episode developed during a Pliensbachian Stage; when a widespread dike swarm was injected, in conjunction with a large number of fissure flow eruptions. Moreover, the identification of more than 2300 bodies of dikes and fractures filled with magmas indicate that the crust was subject to a widespread regional extension accommodating and storing high volumes of rising silica-rich magma at shallower crustal levels. Dikes swarm emplacement can act as a first-order tectonic factor, starting the along-axis continental rift segmentation, e.g., northern Afar rift, in eastern Africa (Wright *et al.* 2006). In this sense, we consider that the mechanism of rifting that acted in the north area could be considered as equivalent to the reported by Wright *et al.* (2006).

However, the magma intrusion via diking does not progress in the same way southern to the E-W Fitarruin Canyon, indicating that the factors that control the regional extension along the CPB are discontinuous or different. The first variation in the extensive dike pattern and the associated volcanism occur southward the trace of the Fita Ruin Canyon (Fig. 12B). The Canyon located at 40º39' parallel in the Río Negro Province forms an E-W elongated valley which extension could be traced in

Journal Pre-proof

continuity with the Loma Blanca dextral fault recognized in La Esperanza area (Corbela, 1975; Giacosa *et al.* 2007). Fault continuity progresses westward along more than 150 km. It has been a remarkable regional dextral strike-slip fault. It extends, following an E-W strike and occurred as a large fault set or fault zone, that we consider naming as Loma Blanca Fracture zone (LBFZ) in the present work.

The faults kinematics was regionally described 40 km NW of Los Menucos town (Giacosa *et al*. 2007), which affected the metasediments of the Lower Paleozoic Colo Niyeu Formation, the Permian granites of La Esperanza and Dos Lomas complexes (Llambías and Rapela, 1984; Martínez Dopico *et al.* 2017) and the Lower Triassic Los Menucos Complex (Labudía and Bjerg, 2001; Lema *et al.* 2008 and Luppo *et al.* 2018). The absence of structural relationships between the LBZ and cretaceous units indicates than the strike-slip faults were active between the Upper Triassic and Lower Cretassic times. The absence of structural relationships between the LBFZ and the Cretaceous units indicate that the strike-slip faults were active between the Upper Triassic and Upper Jurassic periods, and in this sense, active during the Lower Jurassic Period. Although strike-slip structures can also be recognized southern to El Piche Graben, these can be partially differentiated based on the strike attitudes (Fig. 12C).

Southward to the Fita Ruin Canyon, volcanism (CCHC) shows several differences, including lower erupted volumes, a progressive increase of effusive facies, composition, and volcanism type variation. The absence of the regional dikes development also indicates that a shallow magma reservoir does not continue until those latitudes and the massive magma injection, not promoted the south CPB extension in the same way. These changes suggest that the extensional Lower Jurassic phase, in the CPB, can be latitudinally segmented into different areas.

Journal Pre-proof

The regional strike-slip faults that divide the rift into different segments occur as E-W striking structures. These falt systems are interpreted, in the present work, as roughly synchronous with the rift extensión and early evolution. Multiple rifting episodes usually occur in the rift basin, where the segmentation can be promoted during one or more rifting stages. Particularly in the CPB, the relationships between the rift margins and the strike-slip structures are not earliest recognized and neither described although detailed structural análisis was not developed heretofore.

We identify that the main changes in regional volcanism and the related stratigraphy are associated with these regional E-W faults distribution. Also, more than one fault zone can be proposed along the CPB extensión. Locally, the lower erupted volumes southward to the Fita Ruin canyon can be associated with the highest degree of dextral shear stress or changes in the angle of extension as occur in other volcanic rift areas, e.g., Taupo volcanic zone (Spinks *et al*. 2005). The caldera complexes, on the other hand, are develop were the regional extension is roughly orthogonal to the fractures pattern. The segment extension is not entirely clear; regardless, we consider that they have between 40 to 250 km, likewise occurs in different rifted areas around the world.

7. Conclusions

1- The early Jurassic volcanism of Central Patagonia forms an extensive area where the volcanic deposits occur as significant isolated volcanic systems. The composition, depositional, and genetic features show several differences along the strike of the oblique rift distribution. The Cañadón Chileno complex (CCHC), located in the Río Negro province, Argentina, provides the opportunity to evaluate and

Journal Pre-proof

improve the understanding of the Lower Jurassic setting of Central Patagonia since it occurs in the region where these characteristics change.

2- Based on the field and laboratory data developed in the present work, 22 lithofacies were recognized and grouped into eight facies associations. The continental sedimentary environments include alluvial fan deposits (FA 1), ephemeral deposits (FA 2), braided fluvial deposits (FA 3), alluvial plains, or over banks (FA 4), and lacustrine deposits (FA 9). On the other hand, the pyroclastic facies were separated according to the pyroclastic currents involved during the deposition; into fall-out, dilute, and density currents (FA 5, FA 6, and FA 7). Effusive andesitic feeders and lava-flows (FA 8) were also recognized.

3- The stratigraphic data obtained in the present work reveal that CCHC consists of two felsic diatreme volcanoes - described here as Southern and Northern Zone-, developed over a local subsided area, represented by an asymmetrical basin.

4- Seven units were recognized in the CCHC record (Units a, b, c, d, e, f, and g: unit (a) represents an initial stage of continental sedimentation recorded throughout the entire Complex. Unit (b) represents the upper felsic diatreme facies, in Southern Zone of the Complex, where debris flow are interbedded with massive lapilli-tuff deposits. Unit (c) consists of local andesitic lavas flows and feeder dikes, and the unit (d) consists of welded lapilli tuff deposits interpreted as the growth of the volcanic system. The Northern Zone evolves similarly with the felsic intra-diatreme deposits of unit (e).The unit (f) consisting of an effusive stage represented by extended andesitic lava flows. Finally, a deep lacustrine environment is installed (unit g) that includes shallow and deep facies, with intercalations of local pyroclastic deposits.

Journal Pre-proof

5- New geochronological data (U-Pb zircon age of 188 ± 3 Ma) was determined to confirm and reinforce the correlation criteria between the different areas involved, indicating that the volcanism described here is synchronous with the Northern silica-rich calderas of the Garamilla Formation as well as the large andesitic volcanoes of the Lonco Trapial Formation located southward to the CCHC.

6- These changes occur along with the north-south extended areas limited by transfer fault systems developed in continuity strike-slip structures of the La Esperanza area (LBFZ). These changes are relatively constant and regular throughout the entire oblique rift strike, separating differentially structured areas.

Journal Pre-proof

Acknowledgments

This study is part of the research projects “Prospección geofísica de la Provincia de Rio Negro” (grant 24/H061), “Ciclos tectomagmáticos de la República Argentina” (grant 24/H060), and Gondwánico y Patagonídico del Macizo Nordpatagónico occidental (grant 24/H121 and 24H140), granted by the Universidad Nacional del Sur, and the Agencia Nacional de Promoción Científica y Tecnológica-UNS gave a grant to the project “Análisis de la configuración y evolución geológico–geofísica del sector oriental de la Comarca Nordpatagónica” (grant 546).

Finally, Significado y evolución de los eventos tectonomagmáticos Gondwánicos y Patagonídicos del norte de Patagonia (grant 11220150100184) was financed by CONICET.

We thank Antrichipay, Cayupil, Lincopan, and Namur families for allowing access to their lands. Special thanks to people of the Comallo locality, its Major Mr. Raúl Hermosilla, and his family for help during the field trips. We are also profoundly

Journal Pre-proof

grateful for the comments and suggestions made by the Editor-in-Chief Dr. Andres Folguera and the invited Regional Editor, Dr. Cesar Navarrete, and the two anonymous reviewers who provided a detailed critique of the manuscript wich considerably improved its quality.

8. References

Agostini, A., Bonini, M., Corti, G., Sani, F., Mazzarini, F., 2011. Fault architecture in the Main Ethiopian Rift and comparison with experimental models: implications for rift evolution and Nubia–Somalia kinematics. *Earth and Planetary Science Letters*, *301*, 3-4, 479-492.

Autin, J., Bellahsen, N., Leroy, S., Husson, L., Beslier, M. O., d'Acremont, E., 2013. The role of structural inheritance in oblique rifting: Insights from analogue models and application to the Gulf of Aden. *Tectonophysics*, *607*, 51-64.

Bechis, F., Giambiagi, L., Lanés, S., Garcia, V., Tunik, M., 2009. Evidencias de extensión oblicua en los depósitos desinrift del sector norte de la Cuenca Neuquina. Revista de la Asociacion Geologica Argentina, 65, 293-310.

Benedini, L., Gregori, D., 2013. Significance of the Early Jurassic Garamilla formation in the western Nordpatagonian Massif. Journal of South American Earth Sciences, 45, 259-277.

Benedini, L., Gregori, D., Strazzere, L., Falco, J. I., Dristas, J. A., 2014. Lower Pliensbachian caldera volcanism in high-obliquity rift systems in the western

North Patagonian Massif, Argentina. Journal of South American Earth Sciences, 56, 1-19.

Bouhier, V.E., Franchini M.B., Caffe, P.J., Maydagán, L., Rapela, C.W., Paolini, M., 2017. Petrogenesis of volcanic rocks that host the world-class Ag-Pb Navidad District, North Patagonian Massif: Comparison with the Jurassic Chon Aike Volcanic Province of Patagonia, Argentina. Journal of Volcanology and Geothermal Research 338, 101–120.

Branney, M.J., Kokelaar, P., 2002. Pyroclastic density currents and the sedimentation of ignimbrites. In: Geological Society, London, Memoir, 27, 143.

Brune, S., 2014. Evolution of stress and fault patterns in oblique rift systems: 3-D numerical lithospheric-scale experiments from rift to breakup. *Geochemistry, Geophysics, Geosystems*, 15, 8, 3392-3415.

Clifton, A. E., Schlische, R. W., Withjack, M. O., & Ackermann, R. V., 2000. Influence of rift obliquity on fault-population systematics: results of experimental clay models. *Journal of Structural Geology*, *22*, 10, 1491-1509.

Corbella, H. 1975. Hallazgo de un complejo alcalino vinculado a megatrazas de fracturas corticales en la sierra de Queupuniyeu, Macizo Nordpatagónico, provincia de Río Negro, Argentina. 2º Congreso Ibero-americano de Geología Económica, Actas 4: 45-68, Buenos Aires.

Cortiñas, J. S., 1996. La cuenca de Somuncurá-Cañadón Asfalto: sus límites, ciclos evolutivos del relleno sedimentario y posibilidades exploratorias. In Actas *XIII Congreso Geológico Argentino y III Congreso de Exploración de Hidrocarburos, Buenos Aires, Actas,* 147-163.

Costa, R.V., Trouw, R.A.J., Mendes, J.C., Geraldes, M., Tavora, A., Nepomuceno, F., Araújo Jr., E.B., 2017. Proterozoic evolution of part of the Embu Complex,

Journal Pre-proof

eastern São Paulo state, SE Brazil. Journal of South American Earth Sciences, 79, 170-188.

Cristallini, E., Tomezzoli, R., Pando, G., Gazzera, C., Martinez, J., Quiroga, J., Marianso, B.; Bechis, F., Barredo, S., Zambrano, O., 2009. Controles Precuyanos en la estructura de la Cuenca Neuquina. Revista de la Asociacion Geologica Argentina, 65, 248-264.

Cúneo, R., Ramezani, J., Scasso, R., Pol, D., Escapa, I., Zavattieri, A. M., Bowring, S. A., 2013. High-precision U–Pb geochronology and a new chronostratigraphy for the Cañadón Asfalto Basin, Chubut, central Patagonia: Implications for terrestrial faunal and floral evolution in Jurassic. *Gondwana Research*, 24, 3-4, 1267-1275.

Dopico, C. I. M., de Luchi, M. G. L., Rapalini, A. E., Wemmer, K., Fanning, C. M., Basei, M. A., 2017. Emplacement and temporal constraints of the Gondwanan intrusive complexes of northern Patagonia: La Esperanza plutono-volcanic case. *Tectonophysics*, *712*, 249-269.

Figari, E. G., Courtade, S. F., 1993. Evolución tectosedimentaria de la cuenca de Cañadón Asfalto, Chubut, Argentina. In *Actas XII Congreso Geológico Argentino y II Congreso de Exploración de Hidrocarburos,* 1, 66-77.

Figari, C. E., Scasso, R. A., Cúneo, N. R., & Escapa, I. H., 2016. Estratigrafía y evolución geológica de la Cuenca de Cañadón Asfalto, Provincia del Chubut, Argentina.

Franzese, J.R., Pankhurst, R.J., Rapela, C.W., Spalletti, L.A., Fanning, M., Muravchik,M., 2002. Nuevas evidencias geocronológicas sobre el magmatismo Gondwánico en el noroeste del Macizo Nordpatagónico. In *Actas XV* Congreso Geológico Argentino, El Calafate.

Journal Pre-proof

Giacosa, R., Lema, H., Busteros, A., Zubia, M., Cucchi, R., & Di Tommaso, I., 2007. Estructura del triásico de la región norte del macizo nordpatagónico (40º-41ºS, 67º30-69º45O) Río negro. *Revista de la Asociación Geológica Argentina*, *62*, 3, 355-365.

Geraldes, M.C., Almeida, B.S., Tavares Jr., A., Dussin, I., Chemale, F., 2015. U-Pb and Lu-Hf calibration of the new LA-ICP-MS Multilab at Rio de Janeiro State University. In: Geoanalysis 2015. Leoben. Geoanalysis.

Gordon, A., Ort, M.H., 1993. Edad y correlación del plutonismo subcordillerano en las provincias de Rio Negro y Chubut (41°-42°30´ L.S.). In: In *Actas XII* Congreso Geológico Argentino, Mendoza, 4, 120-127.

Haller, M.J., Linares, M., Ostera, H.A., Page, S.M., 1999. Petrology and geochronology of the Subcordilleran Plutonic Belt of Patagonia Argentina. In *Actas II* South American Symposium on Isotope Geology, Carlos Paz, Argentina, SEGEMAR, Buenos Aires, 210-214.

Hauser, N., Cabaleri, N.G., Gallego, O.F., Monferran, M.D., Silva Nieto, D., Armella, C., Matteini, M., Aparicio González, P.A., Pimentel, M.M., Volkheimer, W., Reimold, W.U., 2017. U- Pb and Lu-Hf zircon geochronology of the Cañadón Asfalto Basin, Chubut, Argentina: Implications for the magmatic evolution in central Patagonia, Journal of South American Earth Sciences, doi: 10.1016/j.jsames.2017.05.001.

Houghton, B. F., Smith, R. T., 1993. Recycling of magmatic clasts during explosive eruptions: estimating the true juvenile content of phreatomagmatic volcanic deposits. *Bulletin of volcanology*, *55*, 6, 414-420.

Journal Pre-proof

Lema, H., Busteros, A., Giacosa, R., Cucchi, R., 2008. Geología del complejo volcánico Los Menucos en el área tipo: Río Negro. *Revista de la Asociación Geológica Argentina*, *63*, 1, 03-13.

Lesta, P., Ferello, R., 1972. Región extrandina de Chubut y norte de Santa Cruz. In: Leanza, A.F. (Ed.), Geología Regional Argentina. Academia Nacional de Ciencias, Córdoba, 601-687.

Llambías, E. J., Rapela, C. W., 1984. Geología de los complejos eruptivos de La Esperanza, provincia de Río Negro. *Revista de la Asociación Geológica Argentina*, *39*(3-4), 220-243.

Lorenz, V., 1970. Some aspects of the eruption mechanism of the Big Hole maar, central Oregon. *Geological Society of America Bulletin*, *81*, 6, 1823-1830.

Labudía, C. H., Bjerg, E. A., 2001. El Grupo Los Menucos: redefinición estratigráfica del Triásico Superior del Macizo Nordpatagonico. *Revista de la Asociación Geológica Argentina*, *56*, 3, 404-407.

Luppo, T., de Luchi, M. G. L., Rapalini, A. E., Dopico, C. I. M., Fanning, C. M., 2018. Geochronologic evidence of a large magmatic province in northern Patagonia encompassing the Permian-Triassic boundary. *Journal of South American Earth Sciences*, *82*, 346-355.

McPhie, J., Doyle, M., Allen, R., 1993. Volcanic Textures: A Guide to the Interpretation of Textures in Volcanic Rocks. *CODES, University of Tasmania*, 198.

Miall, A.D., 1996. The Geology of Fluvial Deposits — Sedimentary Facies Basin Analysis and Petroleum Geology. Springer, Berlin, 582.

Mpodozis, C., Ramos, V. A., 2008. Tectónica jurásica en Argentina y Chile: extensión, subducción oblicua, rifting, deriva y colisiones?. *Revista de la Asociación geológica Argentina*, *63*, 4, 481-497.

Navarrete, C., Gianni, G., Echaurren, A., Kingler, F. L., Folguera, A. 2016. Episodic Jurassic to lower Cretaceous intraplate compression in Central Patagonia during Gondwana breakup. *Journal of Geodynamics*, *102*, 185-201.

Navarrete, C., Gianni, G., Christiansen, R., Kamerbeek, Y., Periale, S., & Folguera, A. 2019. Jurassic intraplate contraction of southern Patagonia: The El Tranquilo Anticline area, Deseado Massif. *Journal of South American Earth Sciences*, *94*, 102224.

Nullo, F. E.,1978. *Descripción geológica de la hoja 41d, Lipetrén, Provincia de Río Negro: Carta geológico-económica de la República Argentina, escala 1: 200.000*. Servicio Geológico Nacional. Boletín 158, 88. Buenos Aires.

Nullo, F., Proserpio, C., 1975. La Formación Taquetrén en Cañadón del Zaino (Chubut) y sus relaciones estratigráficas en el ámbito de la Patagonia, de acuerdo a la flora, República Argentina. *Revista de la Asociación Geológica Argentina*, 30, 2, 133-150.

Page, R., S. Page., 1993. Petrología y significado tectónico Jurásico volcánico del Chubut central. Revista de la Asociación Geológica Argentina 43,41-58.

Palladino, D. M., Valentine, G. A., Sottili, G., Taddeucci, J., 2015. Maars to calderas: end-members on a spectrum of explosive volcanic depressions. Frontiers in Earth Science, 3, 36.

Pankhurst, R.J., Leat, P.T., Sruoga, P., Storey, B.C., Rapela, C.W., Riley, T.R., Marquez, M., 1998. The Chon Aike province of Patagonia and related rocks in

Journal Pre-proof

West Antarctica: a silicic large igneous province. Journal of Volcanology and Geothermal Research, 81, 113-136.

Pankhurst, R.J., Riley, T.R., Kelley, S., Fanning, C.M., 2000. Episodic silicic volcanism in Patagonia and the Antarctic Peninsula: chronology of magmatism associated with the break-up of Gondwana. Journal of Petrology, 41, 605-625.

Pankhurst, R. J., Rapela, C. W., Fanning, C. M., Márquez, M. 2006. Gondwanide continental collision and the origin of Patagonia. *Earth-Science Reviews*, *76*, 3-4, 235-257.

Pavón Pivetta, C., Gregori, D., Benedini, L., Garrido, M., Strazzere, L., Geraldes, M., Marcos, P., 2019. Contrasting tectonic settings in Northern Chon Aike Igneous Province of Patagonia: subduction and mantle plume-related volcanism in the Marifil formation. *International Geology Review*, 1-27.

Proserpio, C.A., 1978. Descripción Geológica de la Hoja 42d, Gastre, Provincia del Chubut (1:200000). Servicio Geológico Nacional, Boletín Nº 159, 75, Buenos Aires.

Rapela, C.W., Pankhurst, R.J., Fanning, C.M., Hervé, F., 2005. Pacific subduction coeval with the Karoo mantle plume: the Early Jurassic Subcordilleran belt of northwestern Patagonia. In: Geological Society, London, Special Publications, 246, 217-239.

Riley, T.R., Knight, K.B., 2001. Age of pre-break-up Gondwana magmatism: a review. Antarctic Science, 13, 2, 99-110.

Spinks, K. D., Acocella, V., Cole, J. W., Bassett, K. N., 2005. Structural control of volcanism and caldera development in the transtensional Taupo Volcanic Zone, New Zealand. *Journal of Volcanology and Geothermal Research*, *144*, 1-4, 7-22.

Journal Pre-proof

Strazzere, L., Gregori, D., Benedini, L., Marcos P., Barros, M., Geraldes, M., Pavón Pivetta, C., 2017. The Puesto Piris Formation: Evidence of basin-development in the North Patagonian Massif during crustal extension associated with Gondwana breakup, Geoscience Frontiers, https://doi.org/10.1016/j.gsf.2017.12.019;

Tchamabé, B. C., Kereszturi, G., Németh, K., Carrasco-Núñez, G., 2016. How Polygenetic are Monogenetic Volcanoes: Case Studies of Some Complex Maar-Diatreme Volcanoes. In *Updates in Volcanology-From Volcano Modelling to Volcano Geology*. InTech.

Uliana, M. A., Biddle, K. T., Cerdan, J.,1988. Mesozoic Extensión and the Formation of Argentine Sedimentary Basins. Extensional Tectonics and Stratigraphy of the North Atlantic Margins. *AAPG Memoir*, *46*.

White, J. D., 1996. Pre-emergent construction of a lacustrine basaltic volcano, Pahvant Butte, Utah (USA). *Bulletin of Volcanology*, *58,* 4, 249-262.

White, J. D., Ross, P. S., 2011. Maar-diatreme volcanoes: a review. *Journal of Volcanology and Geothermal Research*, *201*, 1-4, 1-29.

Wright, T. J., Ebinger, C., Biggs, J., Ayele, A., Yirgu, G., Keir, D., Stork, A., 2006, Magma-maintained rift segmentation at continental rupture in the 2005 Afar dyking episode, *Nature*, 442, 291– 294.

Zaffarana, C. B., Somoza, R., 2012. Palaeomagnetism and 40Ar/39Ar dating from Lower Jurassic rocks in Gastre, central Patagonia: further data to explore tectonomagmatic events associated with the break-up of Gondwana. *Journal of the Geological Society*, 169, 4, 371-379.

Zaffarana, C., Gallastegui, G., Lagorio, S., Poma, S., Busteros, A., Varela, S. S., Puigdomenech, C., 2018. Geochemical signature and reservoir conditions of

Early Jurassic calc-alkaline volcanic rocks from Lonco Trapial Formation, Central Patagonia. *Journal of South American Earth Sciences*, *88*, 415-445.

Journal Pre-proof

Journal Pre-proof

Volcanic episode	Influenced area	Geologic Setting	Geologic Unit	Ages	Geochemistry	Authors
V1	Central Patagonia, Río Negro and Chubut provinces	Oblique back arc? (V1)	Garamilla Formation/ Las Leoneras andTaquetrén formations	188-185 Ma	calc-alkaline silica rich volcanism	Franzese *et al.* 2002, Benedini y Gregori, 2013, Benedini et al. 2014
V2		Pull apart (V2) volcanism and sedimentation (Oblique back arc	Lonco Tapial/Cañadón Asfalto formations	177-171 Ma	calc-alkaline intermediate to acidic composition and continental sedimentation	Cúneo *et al* . 2013; Bouhier *et al* . 2017, Hauser *et al.* 2017
V1	Patagonian Andes	Intra arc (V1)	SPB /SCB	187-181 Ma	calc-alkaline gabros to granodiarites	Gordon and Ort, 1994, Rapela *et al* . 2005,
V0, V1 and V2	Eastern Patagonia (Atlantic influence)	Retroarc and plume related volcanism	Marifil Complex	192-177	alkaline to calc-alkaline silica rich volcanism	Cortes, 1984; Alric *et al* . 1999; Rapela *et al* . 2000; Strazzere *et al* . 2017; Pavón Pivetta *et al.* 2019

Journal Pre-proof

Journal Pre-proof

		Lithofacies Code	Lithofacies	Description	Interpretación	Thick (m)
Gravel facies	1	Gmm	Matrix-supported massive gravels	Poorly to non sorted angular blocks floating in a sandy matrix. Massive beds and no clast imbrication. Sharp contacts.	High-stream debris flow in a pre-existing alluvial flow (e.g. channel).	0.5-5
	2	Gcm	Clas-supported massive gravels	Poorly to moderate sorted, sharp base contact	Low energy pseudoplastic debrys flow	0.5-1
	3	Gmg	Matrix-supported gradded gravels	Poorly sorted clasts floating in a sand matrix, showing some normal to inverse gravel clast grading. Sharp contacts	High-stream debris flow in a pre-existing alluvial flow (e.g. channel).	0.5-2
Sandy facies	4	Sm	Medium to very coarse sandstone, sometimes pebbly	Massive sandstones, no structures. Moderate to well sorted.	Sediment-gravity flow deposits	0.1-1
	5	Sh	Horizontally bedded sand	Horizontally laminated, moderate to well sorted sandstones. Parting lineation can occur on the bedding planes.	Plane-bed Flow (critical flow)	0.1-1
	6	Sl	Low-angle crossbedded sand	Low angle cross-bedding dipping b15°. Well to moderate sorted.	Scour fill sandstone	0.1-1
Mud/silty facies	8	Fm	Massive mudstones and siltstones	Massive mudstone non strutured, with desiccation cracks	Deposits from standing pools of water during low stage flood	0.2-2
	9	Fl	Laminated mudstones and siltstones	Fine, laminations.	Waning inter-lobe floods suspention deposits	0.2-0.5
Pyroclastic facies	10, 11	//sL, pmL	Parallel stratified Lapilli and parallel bedded masive Lapillis	Fine to medium grained well sorted Lapilli	Pyroclastic ash fall deposits	0.1-0.4
	12, 13	epmLT, mLT	Juvenile rich eutaxitic masive Lapilli tuff	Masive juvenile rich Lapilli tuff deposits, with quench-cooling textures.	Freato-Plinian deposits	0.5- 20
	14, 15	xsL, xsLT	Cross stratified lapilli and lapilli tuff	Moderate to well sorted low angle stratified lappilli and Lapilli tuff	Dilute pyroclastic density current	0.5-1.5
	16	dmTB	Disorganized, masive tuff Breccia	Disorganized and poorly sorted with subvertical diffuse preferred clast fabrics; contains abundant andesitic and mLT blocks and in a andesitic ash matrix.	En masse deposition of volcanic debris upon syn-eruptive crater floor from dense collapsing columns (Stiefenhofer and Farrow, 2004; Porritt *et al.* 2008)	0.5-20
	17	mTB	masive tuff Breccia	Disorganized and poorly sorted with sub horizontal coarse bedded; contains subangular andesitic block inmersed in a fine grained ash matrix, quench colling textured blocks.	lava flow or lava dome collapse deposits	0.5-5
Efusive facies	18, 19	pfbA, pmA	Porphirithyc flow banded andesite, porphyrithic masive andesite	vertical and horizantal fuidal andesite, feeder or lava coherent facies	lava flow or andesitic feeder	Masive. Flow bands 2-20 cm.
Limestone facies	20	orlM	Organic rich parallel laminated mudstone (limestone)	bituminous organic rich laminated mudstone carbonate	Deep lacustrine limestone	0.5-15
	21	pmnM	Masive with nodular chert mudstone (limestone)	masive mudstone with intense chert nodulus grow	Algal limestones with phreatic silicification	0.5-4
	22	slcM	Stromatolithic laminated mudstone (limestone)	curved, episodic laminated stromatolithic fine limestone with vertical cracks	algal limestone mobil build up with sporadical exposion	0.2-0.5

Journal Pre-proof

Journal Pre-proof

CCHC Stratigraphy Southern Zone sequence	Sub units	Description	Interpretation	CCHC Stratigraphy Northern Zone sequence	Description	Interpretation
Member a		Consists of 40 to 130m thick, continental sedimentary deposits. Form a fining-upw ard sequence. Alluvial fans facies association (FA 1) interbedded w ith ephemeral (FA 2) and overbank deposits (FA 4). Minor Braided facies (FA 3) w ere also recognized.				
	Low er section	140 m thick sequence of planar to slightly-undulatory, low temperature mLT facies (FA 7C), w ith aquifer blocks, quench textures and partill rew orled, interbedded w ith alluvial and sheet flood facies (FA 1 and FA 3). Vertical contact occur in this member	Stratified pyroclastic compoused, Upper diatreme deposits, highly subsided	Member e	Compound massive lapilli tuff (ignimbrite) units (FA 7a) interbedded w ith fines rich sedimentary deposits (FA 4). Consist of three highly-w elded grey to w hite-colored, lithic poor (5-15%), eutaxitic massive lapilli-tuff w ith influence of external Water (fractured-fragments, accretionary lapilli, and microperlitic textures). Thick vary betw een 60 to 140 m, giving a combined thickness of 350 m. Deposits are separated by moderately preserved inter-eruptive fine-grained sediments (FA 4). Discrete levels of surge deposits also occur show ing moderate sorted sets organized in thin parallel beds 1 to 20 cm thick (Lchs and Lctbs) and low angle (< 15 °) cross-stratification (Lxs). The free crystals vary betw een 7 and 15%, w hile accessory lithic fragments are recorded in moderate to high concentrations (18-40%). The morphology is modified by post-depositional processes such as w elding or devitrification or sedimentary influence. Subaerial deposition generate cracked tuff matrix and oxidation.	Stratified pyroclastic compoused, Upper diatreme deposits
Member b						
	Upper section	Is formed by juvenile-rich massive pyroclastic deposits (FA 7a) (45-60 %), w ithout evidence of quench-cooling textures. The thickness increases significantly to the upper section of member (b), as w ell as the juvenile fragment concentration. Deposits are markedly homogeneous, lobe-shaped, scarcely w elded, and develop up to 150m thicknesses	Stratified pyroclastic compoused, Upper diatreme deposits, highly subsided (w all rock debris)	Member f	The low er section is formed by tw o andesitic lava flow s, 150 m-thick, laterally extended, and elliptical funnel-shaped. The upper section, on the other hand, presents tw o extended monolithological (andesitic) massive tuff-breccia (mTBr) interbedded w ith massive lapilli-tuff. The mTBr reaches up to 15 m and has more than 2 kilometers of lateral extension. The origin of mTBr deposits is considered as related to lava collapses and the generation of a block and ash deposit.	Lava-lake, lava grow and collapse (block and ash flow deposits)
Member c		The member (c) is composed of andesitic feeders, lava flow s, and block and ash deposits. The feeders outcrops form sub-rounded and tabular dike-shaped bodies w ith vertical flow bands. Lavas extends for several tens of meters along-strike w ith a thickness that varies from 5 to 20 m. The dikes are fine-grained, brow n to gray colored, and range betw een 0.5 to 2 m (FA 6). The block and ash deposits consist of poorly sorted, monolithological, andesitic, massive tuff-breccia (FA 7b) of 5 to 10 m thick.	Feeder dikes, local lavas, lava grow and collapses	Member g	It consists of a 5-20 m thick discrete eruption or w elded massive lapa-tuff, interbedded w ith silicified and bituminous limestones. Lacustrine facies (FA 9a and FA 9b) reach up 30 m and show shallow and deep facies interbedded w ith minor channelized sandstones beds (FA 9a, FA 9b, FA 4, and FA 3). Show a tabular morphology, strongly dipping (35°), that extends for more than 1 km normal of dip-direction and an elliptical distribution. The chert layers can grow laterally, forming uniform silcretes and massive nodules. Organic matter-rich micrites w ith fetid smell on fresh cuts w ith unidentified plant's remains.The top of the member (f) as a matrix-supported, either non-graded nor stratified, poorly sorted polymictic breccia w ith variable block concentration (30-45%). Polymictic massive disorganized breccia lithofacies form an up-cone shaped outcrop of 2-10 m thick a a diffuse vertical arrangement that gives it a distinctive positive morphology	Minor eruptions related to a deep lacustrine enviroments
Member d		Continous w ith 20 to 30 m of tw o highly w elded juvenile rich ignimbrite units (FA 7a), orange-colored, moderately to poorly sorted, and are separated by thin inter-eruptive fine sediments. Desiccation cracks structured facies reach up to 0.5 m (FA 4a). The first Ignimbrite unit presents a moderatly altered coarse surge deposit at the base (FA 5) formed by 10 m thick parallel to low angle cros stratified lapillis and lapilli-tuff.	Final Southern Zone eruptive stage			

Journal Pre-proof

Journal Pre-proof

Spot number		Pb	Th	U		207Pb/	1 s	206Pb/	1 s		207Pb/	1 s	206Pb/	1 s	207Pb/	1 s	207Pb/	1 s	%
	ƒ 206a	ppm	ppm	ppm	Th/Ub	235U	[%]	238U	[%]	Rhod	206Pbe	[%]	238U	abs	235U	abs	206Pb	abs	Concf
FA 84 C 004	0.00774183	32.7068748	333.659506	1029.8108	0.32400078	0.2076339	12.7303773	0.02832946	12.5410057	0.98512443	0.05315679	2.1876205	180.084435	22.5843992	191.565205	24.3869734	335.495184	7.33936142	53.6772041
FA 84 C 005	0.17522352	5.05244523	34.950274	73.0109511	0.47869906	0.44377973	11.5448947	0.03090892	11.4932316	0.99552502	0.10413155	1.09097314	196.234406	22.5536747	372.914135	43.0525443	1699.02783	18.5359374	11.5498053
FA 84 C 006	0.01202177	13.6099392	288.203192	408.33104	0.7058077	0.19261256	15.4536761	0.02751192	13.0349014	0.84348224	0.05077646	8.30105117	174.957414	22.8055265	178.855994	27.6398261	230.694896	19.1501014	75.8393086
FA 84 C 008	0.00877862	16.4695258	250.7899	517.577921	0.48454521	0.22927772	12.248806	0.02937888	12.0918641	0.98718717	0.05660117	1.95449998	186.659709	22.5706383	209.602249	25.6737727	476.027727	9.30396182	39.2119404
FA 84 C 009	0.02395912	13.2221438	283.654634	373.029249	0.76040856	0.29843511	11.1662821	0.03216469	11.0444093	0.98908564	0.06729291	1.6452596	204.082108	22.5396634	265.177212	29.6104355	846.852254	13.932918	24.0989036
FA 84 C 003	0.20446407	8.84542742	99.1359554	176.801392	0.56071931	0.32434722	12.7086543	0.02818391	12.604565	0.99180957	0.08346562	1.62321758	179.171986	22.5838494	285.241079	36.2503026	1280.12651	20.7792385	13.9964281
FA 84 A 006	0.1209248	1.17428598	20.0683766	41.6395691	0.48195447	0.44185168	7.18516399	0.03022723	5.25361075	0.73117479	0.10601735	4.90164825	191.97026	10.0853702	371.557269	26.6969991	1732.02554	84.8977994	11.0835699
FA 84 A 007	0.19334723	0.98269849	13.0112318	23.2483488	0.55966262	0.47355428	7.18865909	0.02894133	5.59030243	0.7776558	0.11867249	4.51944004	183.919004	10.2816285	393.641024	28.2975113	1936.33236	87.5113801	9.49831791
FA 84 A 008	0.10252721	4.30369274	101.173394	119.895593	0.84384581	0.61462683	6.53044972	0.02866049	5.67448634	0.86892735	0.15553444	3.23217858	182.159315	10.3366054	486.473943	31.7689363	2407.6831	77.8206174	7.56575128
FA 84 B 001	0.06173639	5.1621121	84.5608524	137.01105	0.61718272	0.22837345	6.71091595	0.02944973	2.40233329	0.35797398	0.0562423	6.26619403	187.103403	4.49484734	208.855048	14.0160867	461.946169	28.9464433	40.5032914
FA 84 B 002	0.01467918	6.81804413	129.702121	195.922751	0.66200643	0.22666593	5.66776995	0.02987205	2.26645636	0.39988503	0.05503259	5.19488131	189.747441	4.30054295	207.442617	11.7573703	413.547281	21.4832904	45.8828892
FA 84 B 005	0.08603923	5.5176633	91.7219214	120.960843	0.75827779	0.47976923	3.11029477	0.02971163	2.44419093	0.785839	0.11711286	1.92350311	188.743249	4.61324538	397.914556	12.3763156	1912.62267	36.7893565	9.86829508

Journal Pre-proof

Journal Pre-proof

		Facies association	Facies	Geometry	Interpretation
	FA 1	Alluvial fan FA .	Gmm, Gcm, Gmg and Sm	Tabular to lobe shape bodies with sharp to erosive bases. 1-5 m thick, dominated by pre-eruptive clast population.	Sediment gravity Flow deposited as alluvial fans and ephemeral flows
Lower Member	FA 2	Fluvial ephemeral FA	Gmm, Sm	Concave-up erosive base to tabular, horizontal masive coarse sand bodies and channeled, cut and fill structured	Sandy Sediment gravity Flow deposited as ephemeral fluvial mostly non confined
	FA 3	Fluvial braided FA ?	Sm, Sh, Sr and Sl	Concave-up erosive bases and horizontal to concave-down tops. Bar dimensions vary from 2 to 5 m thick.	Downstream braided bars?
	FA 4	Aluvial plains or Overbank	Fl and Fm	Sheet-like bodies, 0.2-2m thick, complex relations with FA 4	Overbank or interlobe deposition
	FA 5	Direct fall-out dominated pyroclastic FA	//sL, pmL,	Sheet-like beds, 0.2-1.6 m thick, well sorted masive to parallel bedded that mantled the topography	Pyroclastic fall-out deposits
	FA 6	Traction-dominated pyroclastic FA	xsL, xsLT,	Erosive base 0.5m to 2m tabular shaped	Surge or dilute pyroclastic density current deposits
Mieddle member	FA 7 a		mLT, epmLT	Lobe shaped, erosive base, 5 to 200m thick,	Pyroclastic density current main body deposits
	FA 7 b	Granular flow-dominated piroclastic deposits FA	mTB	Lobe shaped, erosive base, 5 to 30 m thick	Block and ash flows related to Dome collapse
	FA 7c		dmTB	cone shaped 3 to 20m thick, vertical arranged to massive	Phreatmagmatic debris Jet breccia
	FA 8	Andesitic lava and vent FA	pmA and fbA	Tabular upper flow banded or horizontal lobe shape bodies	volcanic feeder and lava lake
Upper Member	FA 9a	Lacustrine FA	pmnM, slcM, sh and Gcm	Tabular, 5 to 40 m thick eliptical inwar tilted	Post eruptive shallow lacustrine facies
	FA 9b		orlM,	Tabular 0.5 to 1 m	Deep lacustrine

Journal Pre-proof

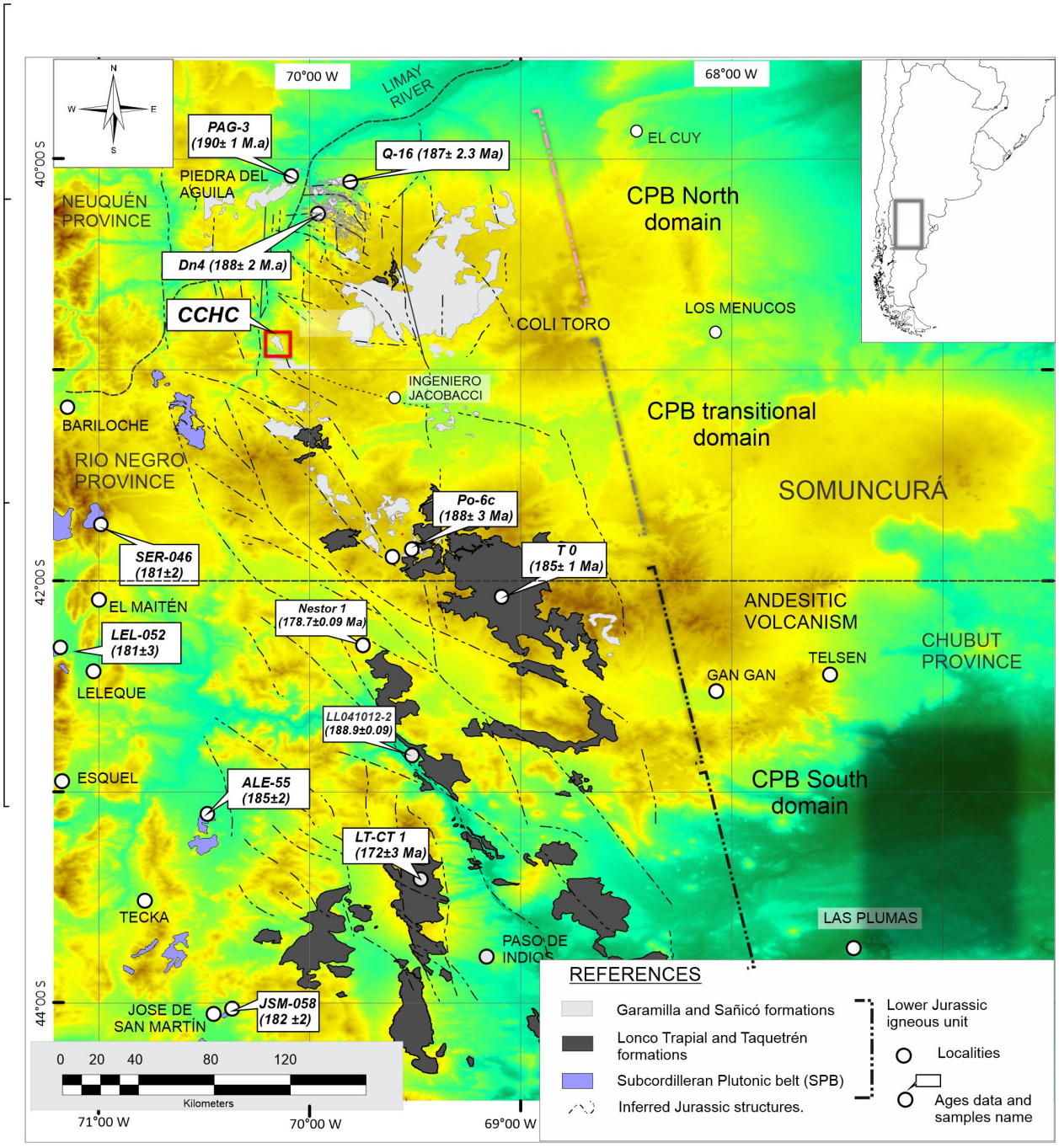
70°00 W
68°00 W
40°00 S
42°00 S
44°00 S
71°00 W
70°00 W
69°00 W
LIMAY RIVER
PAG-3 (190± 1 M.a)
Q-16 (187± 2.3 Ma)
PIEDRA DEL AGUILA
NEUQUÉN PROVINCE
Dn4 (188± 2 M.a)
CCHC
EL CUY
CPB North domain
COLI TORO
LOS MENUCOS
INGENIERO JACOBACCI
BARILOCHE
RIO NEGRO PROVINCE
CPB transitional domain
SOMUNCURÁ
Po-6c (188± 3 Ma)
T 0 (185± 1 Ma)
SER-046 (181±2)
EL MAITÉN
Nestor 1 (178.7±0.09 Ma)
LEL-052 (181±3)
LELEQUE
ANDESITIC VOLCANISM
CHUBUT PROVINCE
TELSEN
GAN GAN
LL041012-2 (188.9±0.09)
ESQUEL
ALE-55 (185±2)
CPB South domain
LT-CT 1 (172±3 Ma)
TECKA
LAS PLUMAS
PASO DE INDIOS
JOSE DE SAN MARTÍN
JSM-058 (182 ±2)
0 20 40 80 120
Kilometers
REFERENCES
Garamilla and Sañicó formations
Lonco Trapial and Taquetrén formations
Subcordilleran Plutonic belt (SPB)
Inferred Jurassic structures.
Lower Jurassic igneous unit
Localities
Ages data and samples name

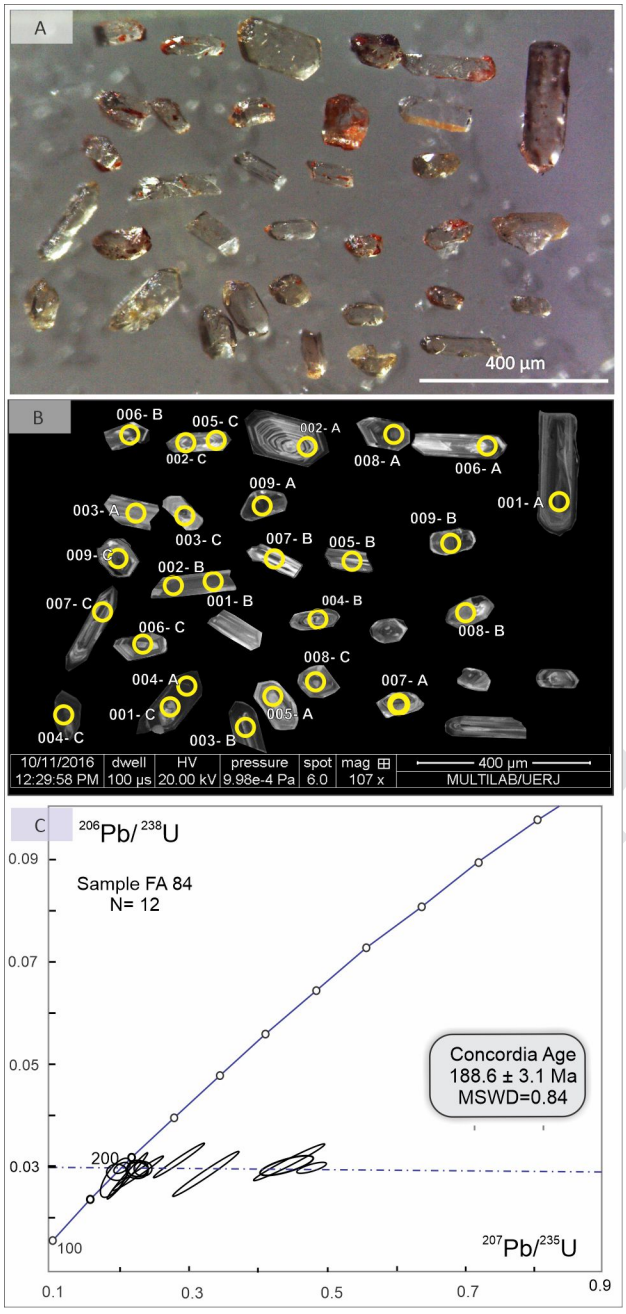
A
400 µm
B
006- B
005- C
002- A
002- C
008- A
006- A
009- A
001- A
003- A
009- B
003- C
007- B
005- B
009- C
002- B
001- B
004- B
007- C
008- B
006- C
008- C
004- A
007- A
001- C
005- A
004- C
003- B
10/11/2016 12:29:58 PM
dwell 100 µs
HV 20.00 kV
pressure 9.98e-4 Pa
spot 6.0
mag 107 x
400 µm
MULTILAB/UERJ
C
206Pb/238U
Sample FA 84
N= 12
Concordia Age
188.6 ± 3.1 Ma
MSWD=0.84
200
100
207Pb/235U
0.09
0.07
0.05
0.03
0.1
0.3
0.5
0.7
0.9

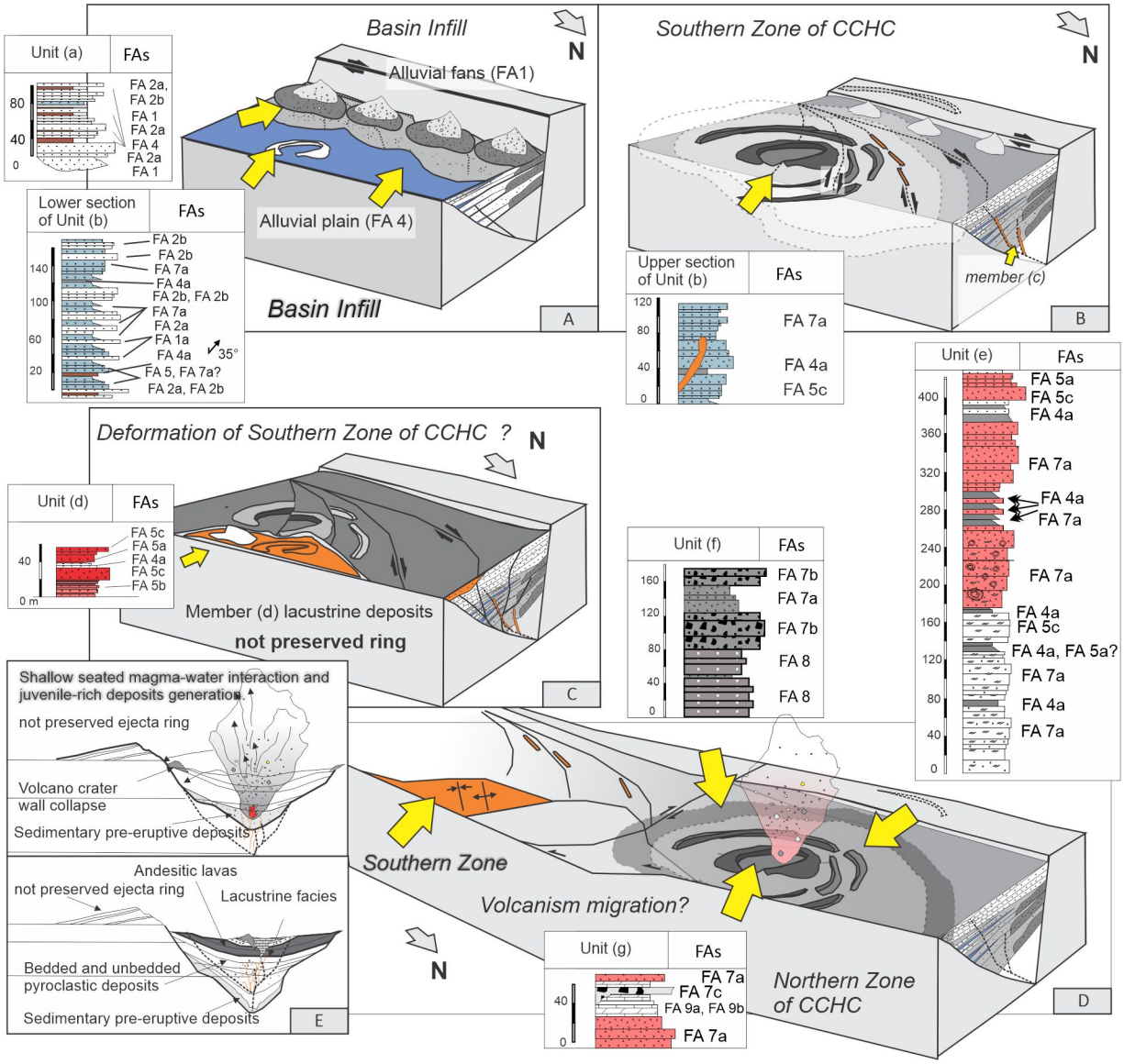
Basin Infill
N
Alluvial fans (FA1)
Alluvial plain (FA 4)
Basin Infill
A
Unit (a)
FAs
80
40
0
FA 2a, FA 2b
FA 1
FA 2a
FA 4
FA 2a
FA 1
Lower section of Unit (b)
FAs
140
100
60
20
FA 2b
FA 2b
FA 7a
FA 4a
FA 2b, FA 2b
FA 7a
FA 2a
FA 1a
FA 4a
35°
FA 5, FA 7a?
FA 2a, FA 2b
Southern Zone of CCHC
N
member (c)
B
Upper section of Unit (b)
FAs
120
80
40
0
FA 7a
FA 4a
FA 5c
Deformation of Southern Zone of CCHC ?
N
Member (d) lacustrine deposits
not preserved ring
C
Unit (d)
FAs
40
0 m
FA 5c
FA 5a
FA 4a
FA 5c
FA 5b
Unit (f)
FAs
160
120
80
40
0
FA 7b
FA 7a
FA 7b
FA 8
FA 8
Unit (e)
FAs
400
360
320
280
240
200
160
120
80
40
0
FA 5a
FA 5c
FA 4a
FA 7a
FA 4a
FA 7a
FA 7a
FA 4a
FA 5c
FA 4a, FA 5a?
FA 7a
FA 4a
FA 7a
Shallow seated magma-water interaction and juvenile-rich deposits generation
not preserved ejecta ring
Volcano crater wall collapse
Sedimentary pre-eruptive deposits
Andesitic lavas
not preserved ejecta ring
Lacustrine facies
Bedded and unbedded pyroclastic deposits
Sedimentary pre-eruptive deposits
E
Southern Zone
Volcanism migration?
N
Unit (g)
FAs
40
0
FA 7a
FA 7c
FA 9a, FA 9b
FA 7a
Northern Zone of CCHC
D

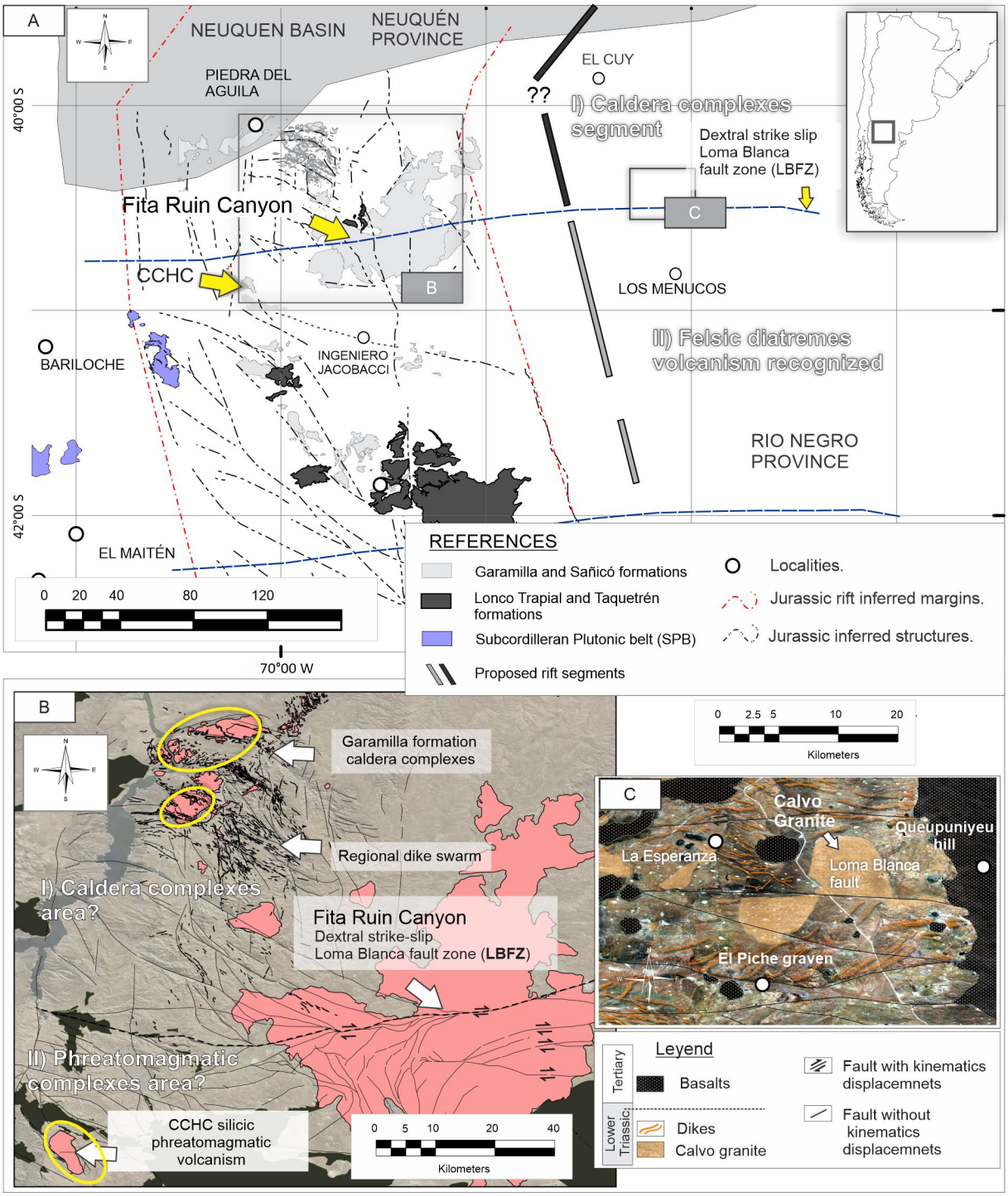
A
NEUQUEN BASIN
NEUQUÉN PROVINCE
PIEDRA DEL AGUILA
EL CUY
??
I) Caldera complexes segment
Dextral strike slip Loma Blanca fault zone (LBFZ)
Fita Ruin Canyon
CCHC
B
C
LOS MENUCOS
BARILOCHE
INGENIERO JACOBACCI
II) Felsic diatremes volcanism recognized
RIO NEGRO PROVINCE
EL MAITÉN
40°00 S
42°00 S
70°00 W
0 20 40 80 120
REFERENCES
Garamilla and Sañicó formations
Lonco Trapial and Taquetrén formations
Subcordilleran Plutonic belt (SPB)
Proposed rift segments
Localities.
Jurassic rift inferred margins.
Jurassic inferred structures.
B
Garamilla formation caldera complexes
Regional dike swarm
I) Caldera complexes area?
Fita Ruin Canyon
Dextral strike-slip
Loma Blanca fault zone (LBFZ)
II) Phreatomagmatic complexes area?
CCHC silicic phreatomagmatic volcanism
0 5 10 20 40
Kilometers
0 2.5 5 10 20
Kilometers
C
Calvo Granite
Queupuniyeu hill
La Esperanza
Loma Blanca fault
El Piche graven
Leyend
Tertiary
Lower Triassic
Basalts
Dikes
Calvo granite
Fault with kinematics displacemnets
Fault without kinematics displacemnets

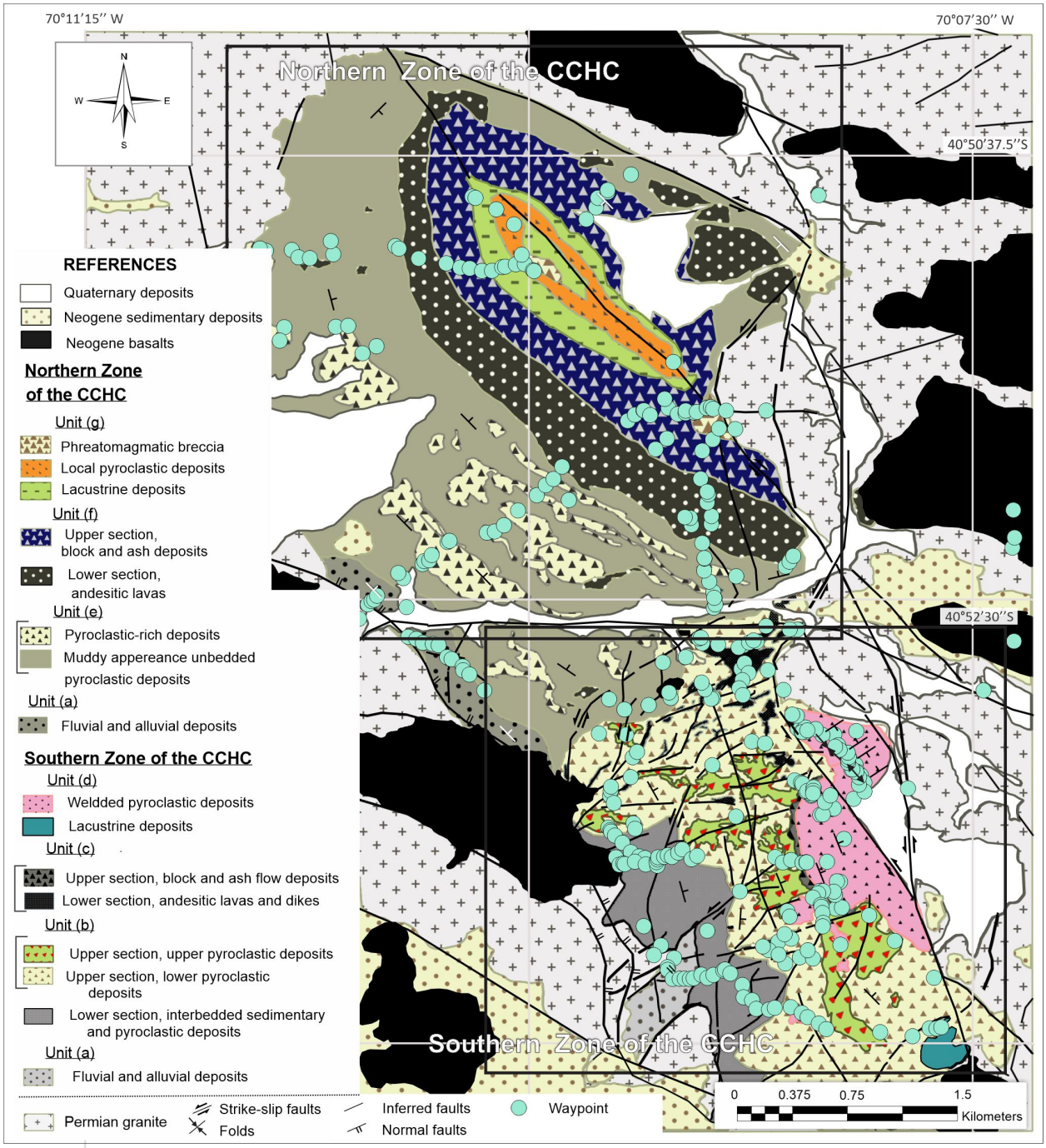
70°11'15'' W
70°07'30'' W
40°50'37.5''S
40°52'30''S
N
W
E
S
Northern Zone of the CCHC
Southern Zone of the CCHC
REFERENCES
Quaternary deposits
Neogene sedimentary deposits
Neogene basalts
Northern Zone of the CCHC
Unit (g)
Phreatomagmatic breccia
Local pyroclastic deposits
Lacustrine deposits
Unit (f)
Upper section, block and ash deposits
Lower section, andesitic lavas
Unit (e)
Pyroclastic-rich deposits
Muddy appereance unbedded pyroclastic deposits
Unit (a)
Fluvial and alluvial deposits
Southern Zone of the CCHC
Unit (d)
Weldded pyroclastic deposits
Lacustrine deposits
Unit (c)
Upper section, block and ash flow deposits
Lower section, andesitic lavas and dikes
Unit (b)
Upper section, upper pyroclastic deposits
Upper section, lower pyroclastic deposits
Lower section, interbedded sedimentary and pyroclastic deposits
Unit (a)
Fluvial and alluvial deposits
Permian granite
Strike-slip faults
Folds
Inferred faults
Normal faults
Waypoint
0
0.375
0.75
1.5
Kilometers

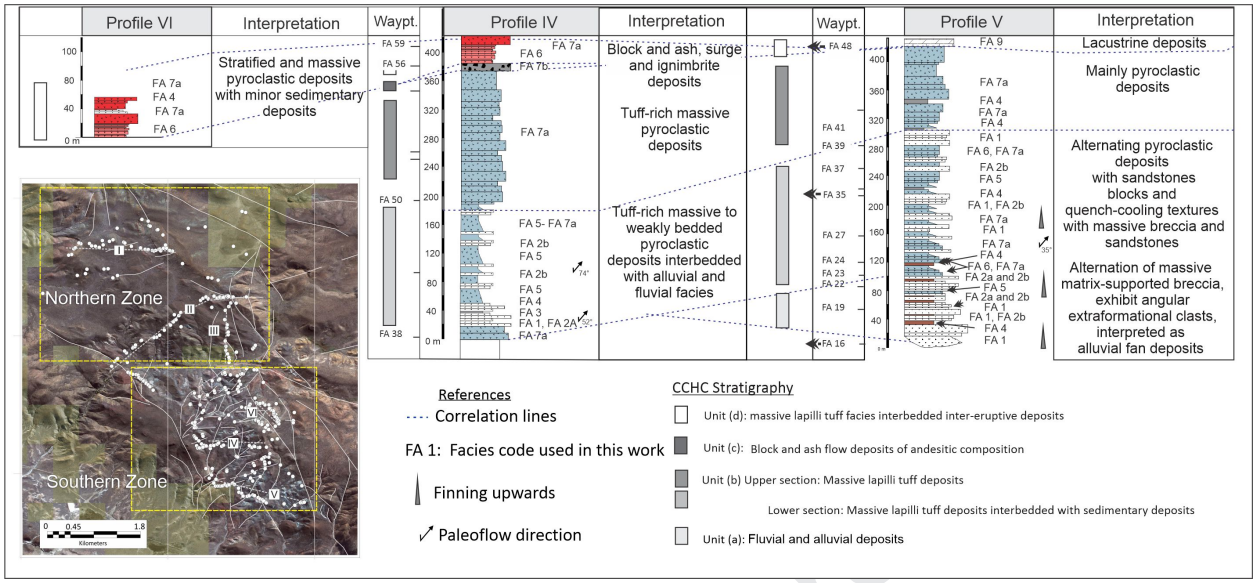

Journal Pre-proof

Journal Pre-proof

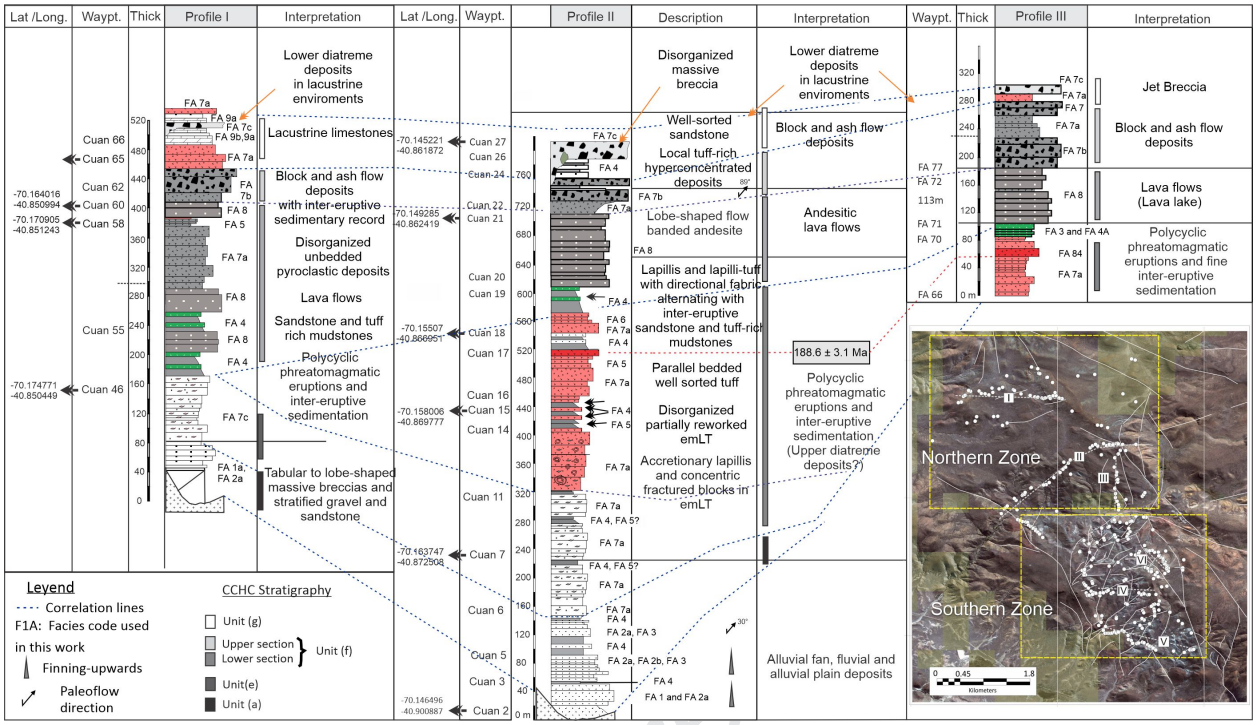

Journal Pre-proof

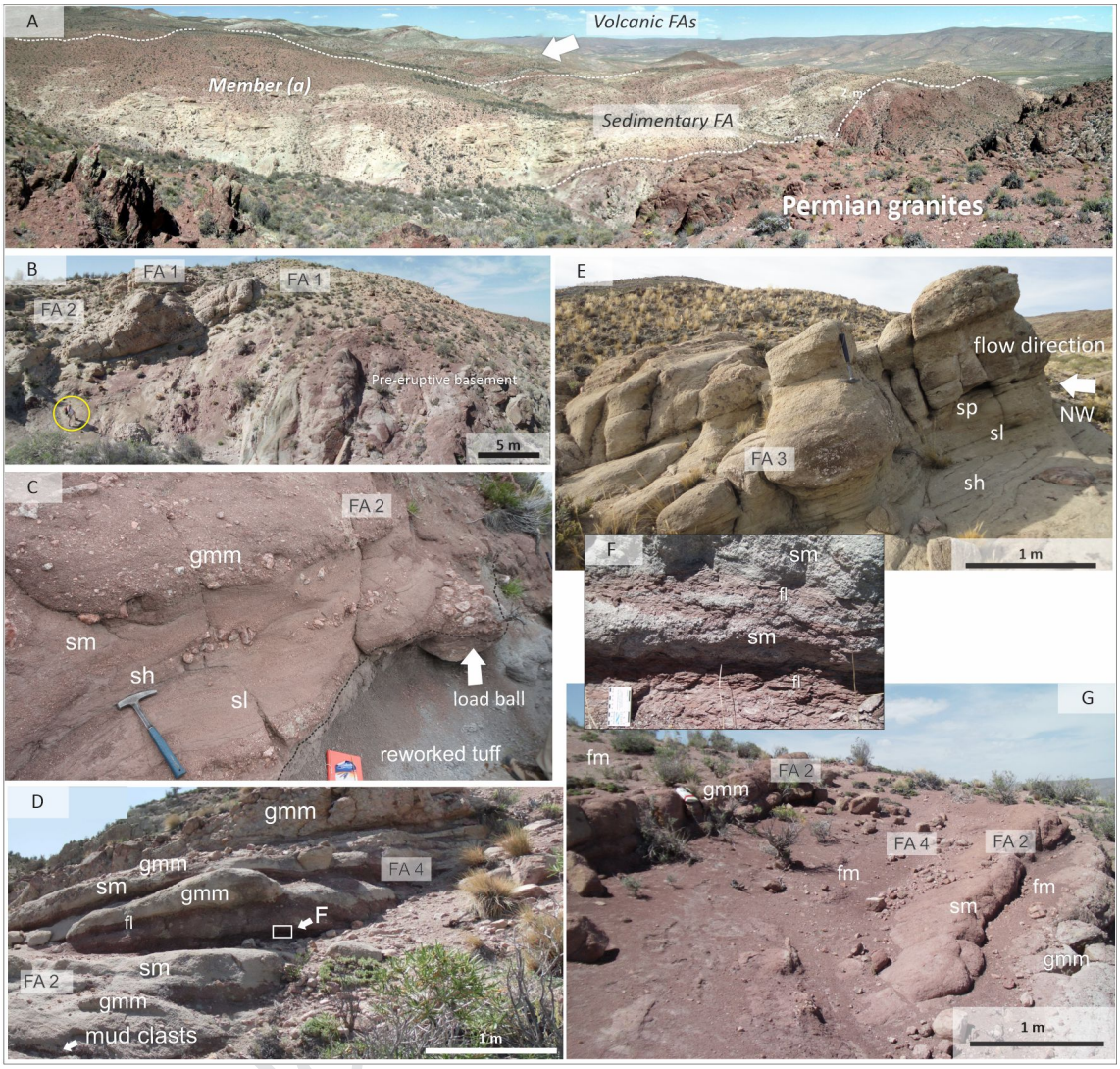
A
Volcanic FAs
Member (a)
Sedimentary FA
Permian granites
B
FA 1
FA 1
FA 2
Pre-eruptive basement
5 m
C
FA 2
gmm
sm
sh
sl
load ball
reworked tuff
D
gmm
gmm
sm
gmm
FA 4
fl
F
sm
FA 2
gmm
mud clasts
1 m
E
flow direction
NW
sp
sl
sh
FA 3
1 m
F
sm
fl
sm
fl
G
fm
gmm
FA 2
FA 4
FA 2
fm
fm
sm
gmm
1 m

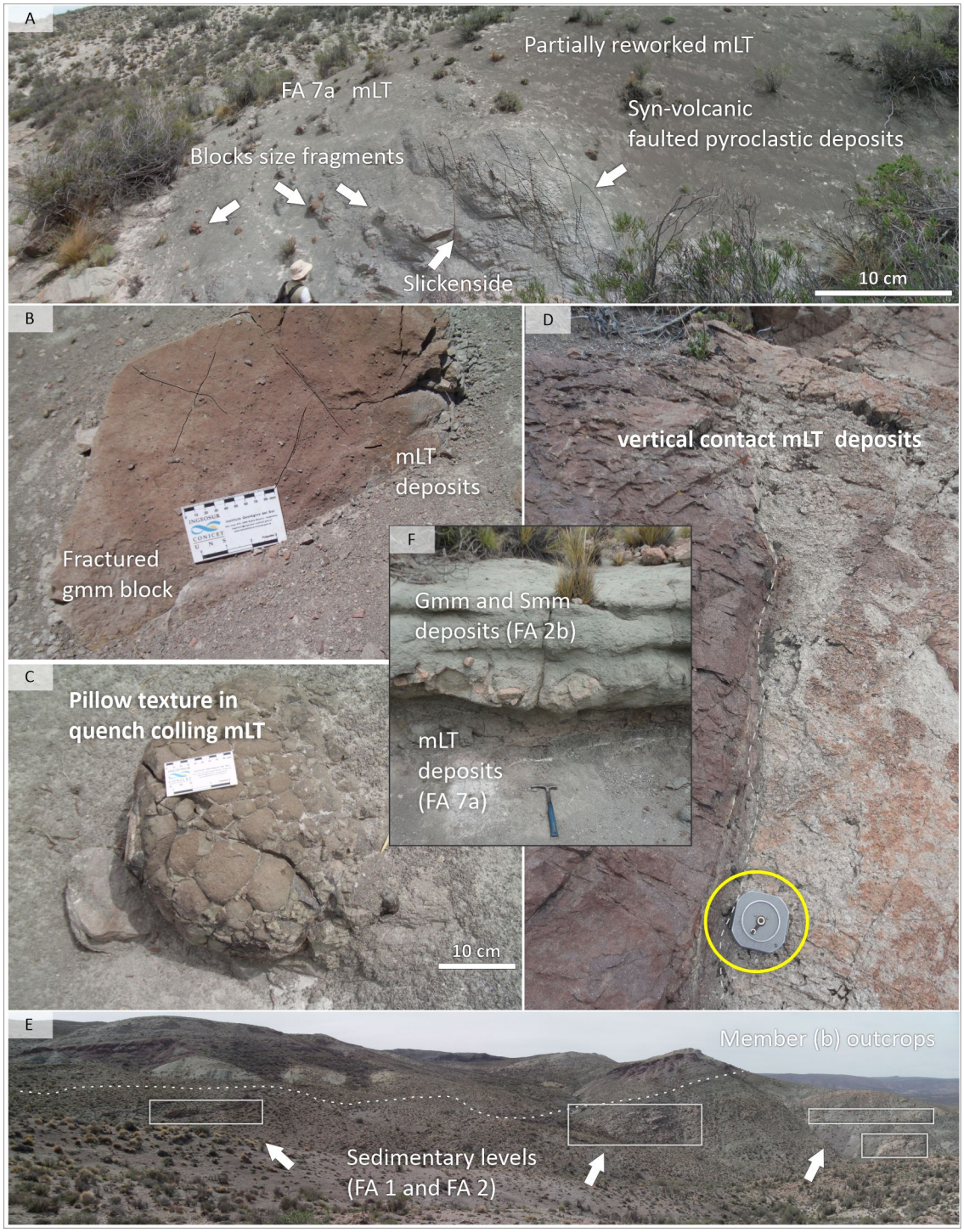
A
Partially reworked mLT
FA 7a mLT
Syn-volcanic
faulted pyroclastic deposits
Blocks size fragments
Slickenside
10 cm
B
mLT
deposits
Fractured
gmm block
D
vertical contact mLT deposits
F
Gmm and Smm
deposits (FA 2b)
mLT
deposits
(FA 7a)
C
Pillow texture in
quench colling mLT
10 cm
E
Member (b) outcrops
Sedimentary levels
(FA 1 and FA 2)


A
Lava lateral flow
Upward flow
10 m
B
Andesitic dike
Tabular morphology
Cooling joints
60 cm
C
Pilotaxic groundmass
Glomerophyric texture
Plagioclase microlites
500 µm
D
Weldded masive lapilli tuff deposits (FA 7a)
Inter-eruptive fine laminated deposits (FA 4)
E
10 cm
F
Altered LT matrix
4 cm

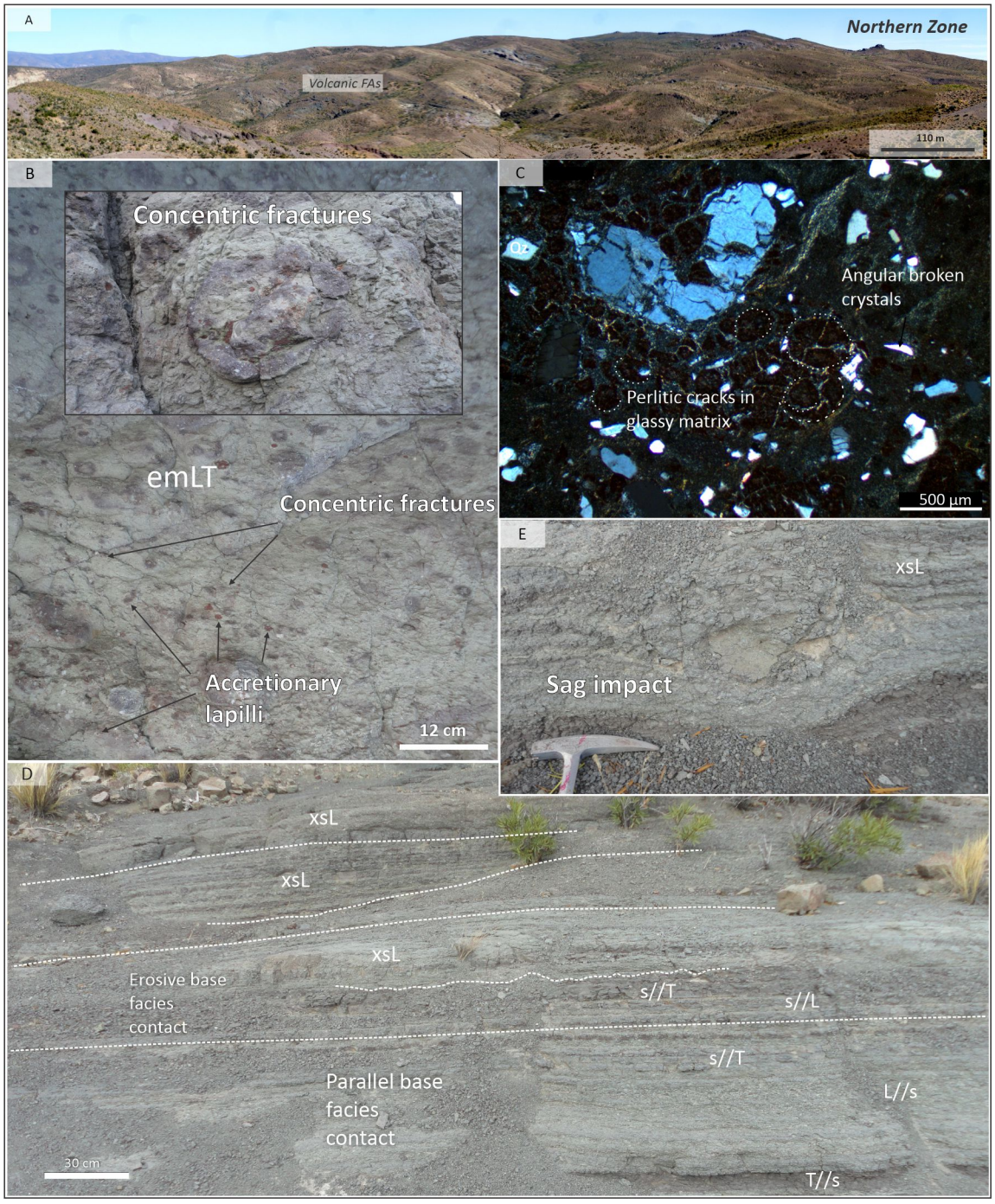
A
Northern Zone
Volcanic FAs
110 m
B
Concentric fractures
emLT
Concentric fractures
Accretionary lapilli
12 cm
C
Qz
Angular broken crystals
Perlitic cracks in glassy matrix
500 µm
E
xsL
Sag impact
D
xsL
xsL
xsL
Erosive base facies contact
s//T
s//L
s//T
Parallel base facies contact
L//s
T//s
30 cm


A
Andesitic blocks
Subhorizontal deposits
Erosive base
C
Laminated limestones
Chert
nodules
Silica filled
fractures
B
Tabular morphology
D
Chert
nodules
Fossil remains
500 µm
10 cm
E
Polymictic disorganized massive breccia, subvertical arrangment

Journal Pre-proof

The Cañadón Chileno Complex (CCHC) is formed by sedimentary and volcanic units.

Includes conglomerates, sandstones, pyroclastic flows, effusive lavas, and lacustrine limestones, assigned to a felsic diatreme volcanism.

The age is 188.0 ± 3 Ma, and is coeval with other units of Patagonia.

Journal Pre-proof

Journal Pre-proof

Bahía Blanca, 26th February 2020

Dear Dr. Andrés Folguera

Editors-in-Chief of Journal of South American Earth Science

Disclosure statement: No potential conflict of interest is reported by the authors.

Thanks in advance. Sincerely yours.

Dr. Leonardo Benedini
INGEOSUR-Departamento de Geología
Universidad Nacional del Sur and CONICET

Journal Pre-proof

Journal Pre-proof

Bahía Blanca, 26th February 2020

Dear Dr. Andrés Folguera

Editors-in-Chief of Journal of South American Earth Science

Disclosure statement: No potential conflict of interest is reported by the authors.

Thanks in advance. Sincerely yours.

Dr. Leonardo Benedini
INGEOSUR-Departamento de Geología
Universidad Nacional del Sur and CONICET

Journal Pre-proof